Journal of Luminescence 255 (2023) 119552

Contents lists available at ScienceDirect

Journal of Luminescence

journal homepage: www.elsevier.com/locate/jlumin

Review

Supported carbon-dots: A review

Orlette Mkhari [a], Themba D. Ntuli [a,b], Neil J. Coville [a,b,**], Edward N. Nxumalo [c], Manoko S. Maubane-Nkadimeng [a,b,d,*]

[a] Molecular Sciences Institute, School of Chemistry, University of the Witwatersrand, Johannesburg, 2050, South Africa
[b] DSI-NRF Centre of Excellence in Strong Materials, University of the Witwatersrand, Johannesburg, 2050, South Africa
[c] Institute for Nanotechnology and Water Sustainability, College of Science, Engineering and Technology, University of South Africa, Roodepoort, 1709, South Africa
[d] Microscopy and Microanalysis Unit, University of The Witwatersrand, Johannesburg, 2050, South Africa

ARTICLE INFO

Keywords:
Carbon dots
Photoluminescence emission
Aggregate-induced emission
Nanocomposites

ABSTRACT

The synthesis of carbon dots (CDs) that are supported on solid matrices to make solid CD-containing composites has emerged as a promising strategy that can be used to circumvent the drawbacks associated with CDs that are made in solution. To date, various solid matrices such as silica, structured carbons, zeolites, titania, xerogels, and carbon polymers have been used to support the CDs, which allows for the realization to make solid CDs/support nanocomposites. The CDs/support or CDs@support nanocomposites have been demonstrated in many instances to have improved properties (that surpass their unsupported counterparts) ranging from enhanced light response, efficient current density, improved photostability, suppressed nonradiative recombination, enhanced electron-hole pair separation, higher quantum efficiencies, enhanced electron transfer rate, and upconversion photoluminescence properties. In addition, supporting CDs onto a solid matrix can simplify the CD purification processes, lead to better reusability, reduce aggregate formation and also impact on the hygroscopic nature of the CDs. The improved properties that have been demonstrated in CDs/support nanocomposites have opened doors for application in various fields such as photocatalysis, electrochemistry, optics, nanomedicine, sensing, adsorption, and bioimaging, among others. Hence, this review describes the synthesis, properties, importance, and role of CDs/support nanocomposites in various applications.

1. Introduction

Carbon dots (CDs) are one of the recently described structured carbon-based nanomaterials with a zero dimension. Since their discovery, CDs have drawn much attention as a new member of the carbon nanomaterial family [1]. CDs were first identified as carbon nanoparticles and later called CDs, as they showed similar properties to the well-studied inorganic quantum dots [2]. Structurally, CDs are usually spherical and are made of sp^2/sp^3 hybridized carbon atoms, attached to oxygen, hydrogen, and nitrogen, mainly on their surface [2,3]. They were accidently discovered by Xu et al., in 2004 during the electrophoretic purification of single-walled carbon nanotubes obtained from arc-discharge soot and were found to have a composition of 53.93% C, 2.56% H, 1.20% N, and 40.33% O [4,5]. As shown in Fig. 1, CDs are zero-dimensional carbon-based nanomaterials (diameter ≤10 nm) [6] with the particle surface functionalized by organic molecules or coated with polymers or other species [7,8]. Generally, four types of CDs have been synthesized, and these carbon nanoparticles can be grouped into graphene quantum dots, carbon quantum dots or carbon nanodots, and polymer dots [9,10].

Although these CDs have similar core structural components involving sp^2/sp^3 carbon atoms, they can be distinguished as follows: graphene quantum dots (GQDs) primarily consist of small graphene fragments made from nano-sized graphene sheets with lateral dimensions being larger than their height. In contrast, carbon quantum dots (CQDs) are spherical shaped nanoparticles with a crystalline carbon core, carbon nanodots (CNDs) are well-carbonized nanoparticles that are neither crystalline nor polymeric and carbonized polymer dots (CPDs) primarily consist of π-conjugated polymers and show no quantum confinement effects due to their particle size [11,12].

In comparison to traditional semiconductor quantum dots based on metallic elements such as CdS, CdSe, PbSe, and Ag_2S [13], CDs have

* Corresponding author. Molecular Sciences Institute, School of Chemistry, University of the Witwatersrand, Johannesburg, South Africa.
** Corresponding author. Molecular Sciences Institute, School of Chemistry, University of the Witwatersrand, Johannesburg, South Africa.
E-mail addresses: neil.coville@wits.ac.za (N.J. Coville), manoko.maubane@wits.ac.za (M.S. Maubane-Nkadimeng).

https://doi.org/10.1016/j.jlumin.2022.119552
Received 9 September 2022; Received in revised form 3 November 2022; Accepted 22 November 2022
Available online 23 November 2022

unique and advantageous properties such as water dispersibility [4], luminescence [2], inexpensive preparation methods, low toxicity, diverse intrinsic electronic and magnetic properties, chemical diversity, high electron transfer rates, and biocompatibility, that make them attractive for many applications [14,15]. Their superior luminescence emission properties, which exceed that of other organic and inorganic quantum/semiconductor nanodots, have contributed to the exponential growth in their exploration [16]. In addition, CDs have been confirmed to show multiple photon-absorptions/emissions (affected by solvent polarity, pH changes, and support matrices) which can facilitate their upconversion photoluminescence properties. In this process, low excitation energy can be converted by electronic transitions into high energy emissions. This property has led to their exploration of possible applications in fields such as drug/gene delivery, biological imaging, antibacterial and antioxidant activity, and sensing applications. They have thus been used in photoluminescence sensors, electrochemiluminescence sensors, electrochemical sensors, catalysis, water treatment, sensing devices, solar energy, bioimaging, drug delivery, nanomedicine, optronic devices, and multi-imaging [2,17,18].

Not unexpectedly they also have limits to their use. For example, their strong fluorescent emissions (due to resonance energy transfer or direct $\pi \rightarrow \pi$ interactions) can be drastically reduced or quenched, when the CD is transferred from a solvent to the solid phase [19,20]. The aggregated-induced quenching of their luminescent emissions and the excessive hygroscopicity of CDs are thus major shortcomings that still need to be addressed, especially in the fields that require solid-state photoluminescent emission [20]. In addition, the ultra-small size of CDs makes them difficult to separate from the solvent in which they were made, which also poses questions regarding their reusability [21,22]. Some of these shortcomings can be overcome by passivation of the CD surface using polymeric materials, functionalization, and/or doping with heteroatoms such as N, O, B, and P.

An alternative and promising way to overcome these drawbacks (formation of aggregates, quenching of fluorescent properties) is to make CDs that are bound to a solid support. To address these problems, many solid/porous matrices have been used to support and modify the properties of CD. They include carbon nitride [23], porous carbon spheres [24], Fe_3O_4@solid-carbon-spheres [21], carbon polymers [25], mesoporous silica [26], cyclodextrin decorated chitosan [27] and polyvinyl alcohol films [28]. Herein, we have appraised the effect of the support on the properties of CD/support nanocomposites. In doing so, we have paid attention to specific features of the CD/support materials, viz. their synthesis, properties, applications, drawbacks, mitigations, and the use of these CDs supported on different matrices. In this way, we hope to indicate the potential of CD-supported nanocomposites as a way forward in the area of CD science.

2. Synthesis of carbon dots

The synthesis of CDs can follow two different strategies; namely: bottom-up and top-down approaches (Fig. 2) [29]. These methods have been summarized in many excellent reviews and details of the approaches can be found elsewhere. The bottom-up approach makes use of carbon-containing molecules as the starting reagent, usually synthesized by pyrolysis or carbonization methods [29,30]. The various methods used result in producing CDs with well-defined shapes and sizes [6,8]. The top-down approach uses larger carbon materials (e.g., graphite and carbon nanotubes) as starting materials, which are then broken down into CDs via chemical, physical or electrochemical means [31]. Some of the synthesis methods that are used for the preparation of CDs are summarized below. To date, CDs have been prepared from many different carbon sources such as biomass, organic solvents, and graphitic carbon particles [32,33].

One of the commonly used bottom-up approaches for the synthesis of CDs is the hydrothermal method. In the hydrothermal method, CDs can be made from a wide range of starting materials under mild

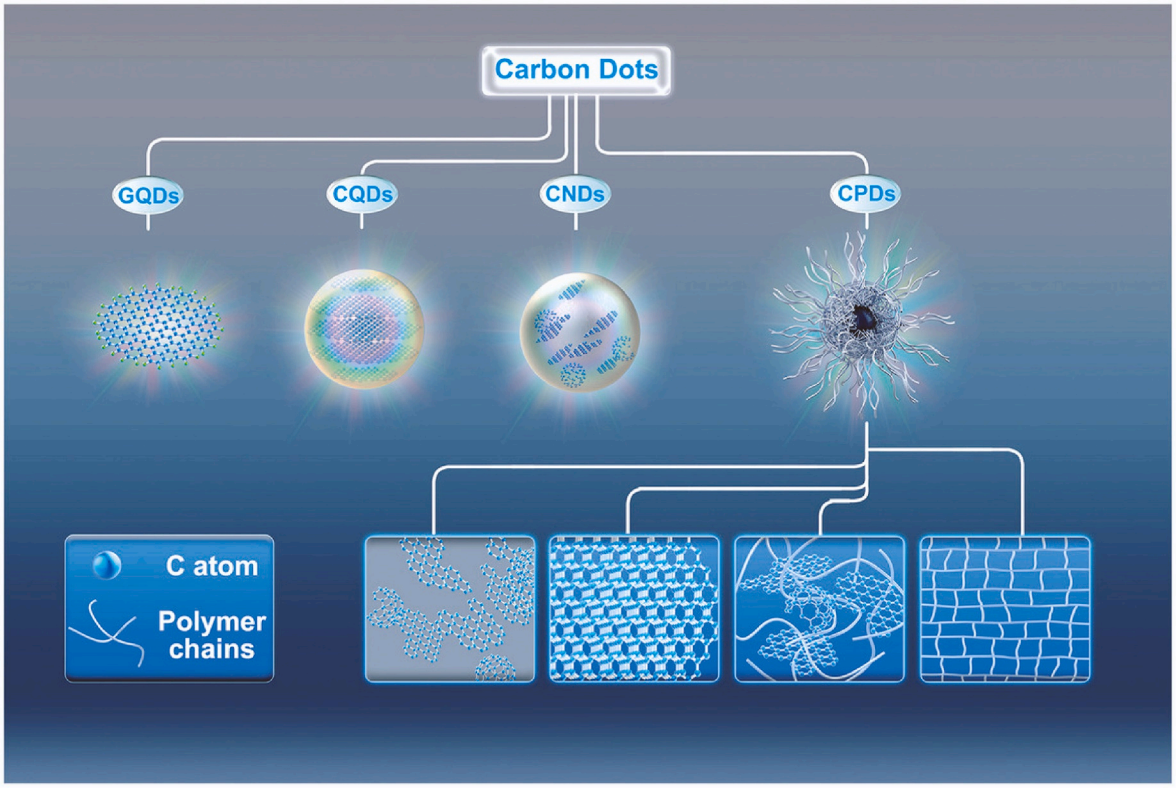

Fig. 1. Types of carbon dots, graphene quantum dots (GQDs), carbon nanodots (CNDs) or carbon quantum dots (CQDs) (depending on their crystallinity) and carbon polymer dots (PDs), (Adopted with permission from Wiley-VCH, copyright 2019) [11].

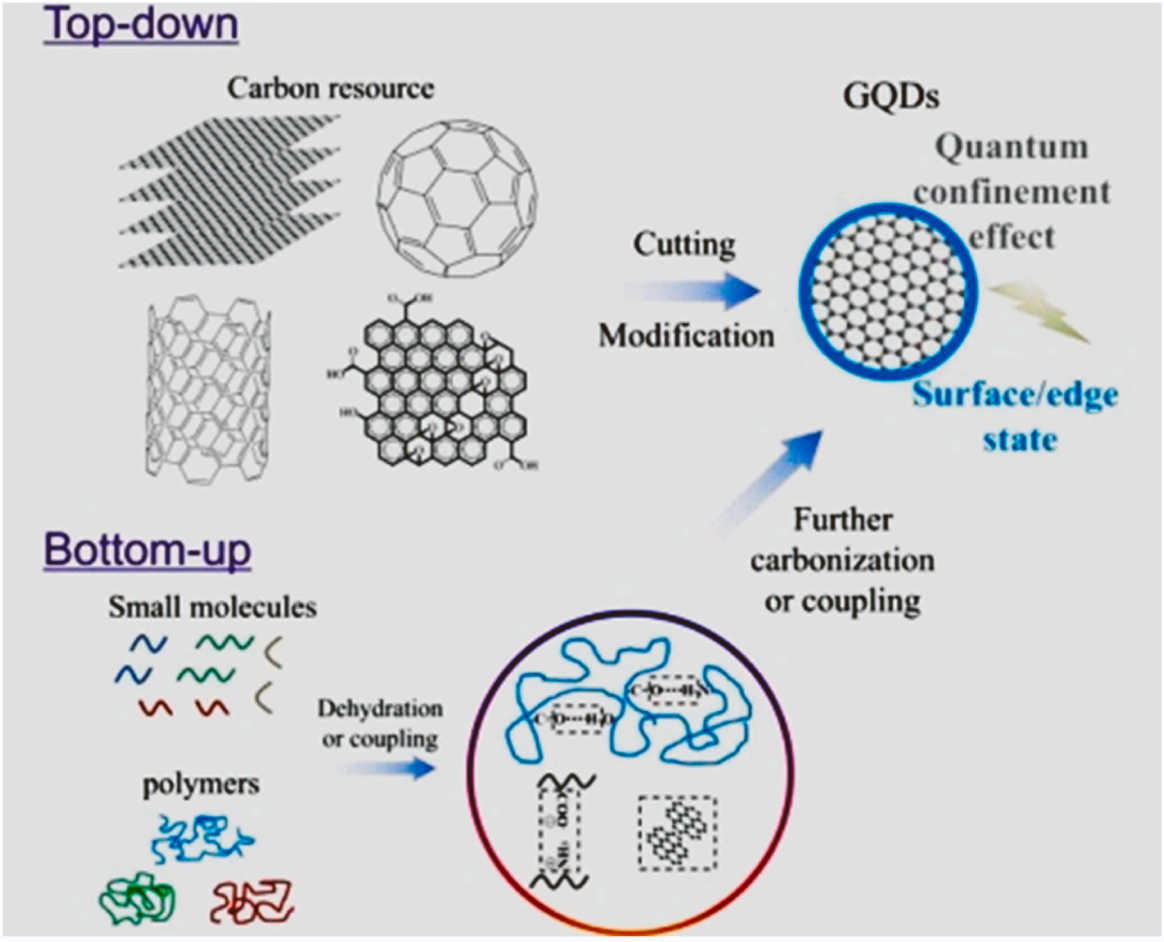

Fig. 2. Two main approaches have been adopted to prepare fluorescent GQDs: the "top-down" route from different carbon sources and the "bottom-up" method from small molecules or polymers, (Adopted with permission from Elsevier B.V. copyright 2017) [29].

temperatures (100 °C–240 °C) and at high pressure. The methods typically used to make CDs by the top-down approach include chemical ablation. In the chemical ablation method, small carbon molecules are turned into carbonaceous materials by using strong oxidizing acids. For example, the hydrothermal oxidation of nano-diamond with concentrated sulfuric acid, $NaNO_3$, and $KMnO_4$ was used for the synthesis of carbon dots with tunable photoluminescence properties [34]. Although the method can produce carbon dots in modest yield, the use of strong oxidizing agents is a drawback and thus the method has received minimal attention for the synthesis of CDs.

3. Properties of carbon dots

Optical absorption: The structural makeup of the CDs makes them an excellent photon harvester in the short-wavelength region (UV–vis region). Typically, the π-conjugated electrons in an sp2 atomic framework are known to exhibit excellent absorption in the UV region (230–320 nm). In essence, there are two common absorption peaks, at ~230 nm and at ~300 nm, which originate from a π-π* and n-π* transition of aromatic C═C bonds and C═O bonds. It should be noted that the particle size, surface states, and passivation agents can influence the absorption characteristics of the CDs [35]. For example, varying the ratio of citric acid and 1-(2-pyridylazo)-2-naphthol, the carbonization temperature, and the reaction time to make CDs resulted in CDs with different surface states (hydrophilic and hydrophobic groups) which then exhibited unique absorption behavior between 250 and 500 nm [36,37]. Other than focusing on the UV region absorption region, an effort has been made to synthesize CDs with deep-red/near-infrared absorption for use in biomedical applications. This long-wavelength absorption region can be achieved by varying CDs morphology, chemical composition, and surface states among others [38].

Fluorescence emission: The study and use of CDs have gained momentum due to their photoluminescence emission properties which exceed those of other organic and inorganic quantum/semiconductor nanodots [16]. The photostability, non-blinking photoluminescence (PL), and light absorption over a wide range give CDs merit over other organic fluorescent materials. Fig. 3 shows the typical photoluminescent emission spectra of CDs [39]. The PL spectra can be used to calculate the quantum yield (QY) of CDs [17]. Interestingly, factors such as particle size and distribution, surface passivation, functional groups, synthesis

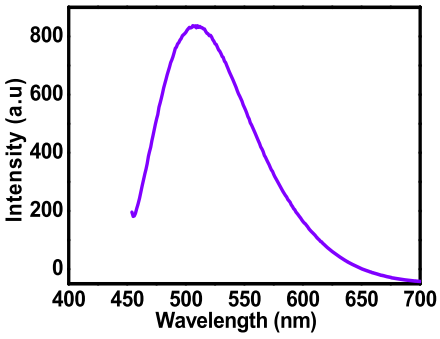

Fig. 3. Typical photoluminescence spectra of CDs, (Adopted with permission from Elsevier B.V, copyright 2021) [40].

method, and reagents used all influence the fluorescent emission [31]. A typical characteristic of photoluminescence in CDs is their excitation wavelength-dependency in which their emission profile is known to strongly depend on the energy package used for excitation. Studies have demonstrated the possibility of excitation-independent characteristics in CDs, which relates to their homogeneous particle size distribution [17,18].

Biocompatibility: Due to their biocompatibility, CDs have been tested on various tissues, organs, and mice tumors for biological applications. They were used for the visualization and identification of healthy cells and to differentiate them from tumor cells. So far, various drug delivery studies on tissues, cells, and organs have been conducted and have shown that CDs are biocompatible with low to no toxic effects on healthy cells [41]. Recently, Liu et al. demonstrated the biocompatibility of CDs derived from mulberry leaves by feeding the CDs to silkworms. The eggs that were laid also exhibited fluorescence emission, but the fluorescence characteristics were not passed to the second generation. Most importantly, the study demonstrated the biocompatible and non-toxic nature of CDs [42].

Electrical: CDs have a high rate of electron transfer which results from the conjugation in its carbon core, abundant functional groups, and hetero-atom dopants [43]. CDs derived from commercial sugar were synthesized using microwave-assisted techniques. It was observed that their electronic transitions were greatly influenced by the concentration of the CDs. For example, it has been shown that the CDs core and surface energy transitions on absorption spectra were dependent on the CDs concentration. As the concentration was increased the surface energy become more dominant than the core energy, which further resulted in a shift in absorption spectra. In essence, as the concentration of the CDs was increased the distance between neighboring CDs was reduced and the surface states overlapped to generate new energy levels which in turn caused red shifts [44]. These observations were further substantiated using photoluminescence spectroscopy and time-resolved photoluminescence spectroscopy.

4. Shortcomings of carbon dots

Origin of PL emission: Regardless of their promising potential applications, research on CDs is still at an infant stage. The mechanism that leads to their photoluminescence emissions and their mechanism of action when interacting with biological systems is still not fully understood. Some reports have shown that the mechanism of action for optical absorption and fluorescence emissions in CDs does not originate from a bandgap, but instead is due to the π-plasmon and radiative recombination of the surface-confined electrons and holes. This would be a different process from that shown by the semiconductor quantum dots [43,45]. Thus, their excitation wavelength dependency in fluorescent emission has been proposed to be due to quantum confinement (particle size), surface states (functional groups), and the chemical properties of the carbon core. Solvatochromism studies offer a platform for identifying the main components responsible for PL emission in CDs. These methods have explored the effect of solvent polarity on the PL emission of CDs. So far, solvents with high polarity have been observed to exhibit redshift emission and this was suggested to be due to hydrogen bonding and dipole-dipole interactions between surface states in the CDs and the solvent [46]. Although there are extensive studies on solvatochromism much work to elucidate the mechanism involved in the PL emission of CDs is needed.

Purification steps: Their small size (≤10 nm) makes it difficult to separate CDs, especially when in solution. This is because during their synthesis other carbon residuals with various particle sizes and shapes are formed and separating them from the CDs is a challenge. Separation of CDs from residuals requires multi-steps that include filtration, centrifugation, micro-filtration, and dialysis. In addition, obtaining solid-state CDs is difficult because they absorb moisture and mostly remain as a gel. Freeze-drying can often be essential in obtaining solid-state CDs products.

Aggregation: In their solid form, CDs tend to agglomerate and result in compromised fluorescent emission, which can result in self-quenching or aggregate-induced PL quenching [28]. As a result, removing solvent from the CDs to obtain them in the solid state can result in tuning or quenching of their PL emission profile which limits their application, especially in the fields that require them in the solid state [47].

Functional groups: The abundant functional groups on CDs have been reported to be responsible for the PL emissions of the CDs, which implies that changing the chemical environment can result in an alteration of their PL emission profile. Unfortunately, the abundant surface functional groups can decompose at a temperature below 250 °C resulting in the formation of larger carbon structures suggesting that their applications are sensitive to temperature and can not be applied in fields that require high-temperature operations [40,48].

5. Modification of the PL properties of carbon dots

Surface passivation: Passivation agents such as polymeric materials have been used to form a thin insulating layer that protects the surface of the CDs. Passivation can be beneficial since it inhibits contamination of the CDs surface while maintaining its functional properties [49]. Passivation of CDs using diamine-terminated oligomeric poly (ethylene glycol) resulted in strong photoluminescence emission under UV lamp illumination at 365 nm, with a reasonable quantum yield of about 14.7% [50].

Functionalization: The introduction of various functional groups such as amines, carbonyl, and hydroxyl functionalities on CDs can result in the generation of new surface states that can act as electron traps or adsorption sites and can induce fluorescent emission. The acid treatment approach was used to introduce functional groups such as carbonyl and carboxyl, while a one-pot reaction of a carbon nitrogenated precursor was used to introduce nitrogen functional groups onto the CDs surface [6,50]. These functional groups play a major role during applications in which they can act as adsorption sites, electron traps, PL emission moieties, or can act as reducing/oxidizing agents for adsorbed metal ions.

Doping: Doping involves the introduction of impurities into a pure natural matrix or compound. CDs have been doped with various heteroatoms such as N, O, B, and P, which have been found to modify their electronic and optical properties [51–53]. Doping can be achieved via the one-pot synthesis or a post-modification method. In most cases, doped CDs have been reported to have improved properties when compared to their undoped counterparts.

It is without a doubt that the introduction of surface passivation, surface defects, functional groups, and doping with heteroatoms can greatly influence the optical properties of the CDs. The in-depth discussion on how the modification of particle sizes, carbon core, defects, and surface functional groups influences the optical properties of CDs can be found elsewhere [54].

Solid support **matrix:** Supporting the CDs on a solid matrix has been observed to overcome the shortcomings that are experienced in controlling the properties of CDs. The types of matrices that have been used for supporting CDs are discussed below:

5.1. CD/support and CD@support nanocomposites

Supporting CDs (CDs/support or CDs@support) on a solid matrix has been used as an alternative strategy to prevent aggregate-induced quenching of fluorescent emissions. The strategy is also used to simplify purification steps, and to improve CD properties such as adsorption, light capture, and electron transfer. Different procedures have been used to create the CD-support composites. For example, the CDs can be added to a silica matrix to give CD/SiO_2 materials. The CDs could be placed on the surface or in the pores of the support. Secondly, the CDs can be covered or partially covered by a support e.g. silica

(made from soluble silica precursors) to generate CD@SiO_2 nanocomposites. The former method also has an unexpected effect in that it can be used to introduce various functional groups onto the support (via the CD functional groups) and could thus reduce agglomeration of the support itself [55]. To date, various supports such as CNTs, carbon nitrides, hollow carbon spheres, solid carbon spheres, titania, metal oxides, polymers, metal nanoparticles, and noble metals, among others have been utilized to enhance the properties of CD/support composites. Generally, four approaches can be used to obtain the CD/support nanocomposites, (i) CDs and support matrices can be synthesized separately, and the two components combined, (ii) CDs can be synthesized separately and then the support matrix precursor coated onto the already synthesized CDs, (iii) the support matrix synthesized synthesized followed by infiltration or dispersion of CD precursors, and (iv) the CDs and support matrix precursors are mixed to give the CDs-support nanocomposites at the same time [40,56,57].

For example, Shanker et al. incorporated the pre-synthesized CDs (graphene quantum dots) into the exfoliated g-C_3N_4 using a hydrothermal method in an autoclave reactor at 120 °C for 2 h to generate a CDs/g-C_3N_4 nanocomposite. The nanocomposite was used as a photocatalyst system for the photodegradation of 4-bromophenol [58]. Liao et al. demonstrated the ternary fabrication of a TiO_2/CDs/Au nanocomposite by combining the pre-synthesized CDs and electron-oxidized TiO_2 via an annealing method in a muffle furnace at 450 °C for 3 h. The obtained nanocomposite was used for photoelectrochemical water-splitting reactions [59]. In these studies, there was no formation of covalent bonds existed between CDs and the support matrices but strong interfacial interaction that resulted in the improved properties of the composites.

In contrast, Mou et al. demonstrated the possibility of covalent bond formation between pre-synthesized CDs and g-C_3N_4. This was achieved by mixing urea (precursor for g-C_3N_4) and a pre-synthesized CDs solution under stirring for 2 h. Thereafter, the solvent was evaporated at 100 °C which was followed by thermal pyrolysis at 550 °C for 3 h to obtain CDs/g-C_3N_4 nanocomposite that was covalently linked by tris-s-triazine units through N–C bonds (π-p-π network) [60]. Yan et al. used a one-step solvothermal method in an autoclave reactor at 200 °C for 8 h to obtain Si/CDs nanocomposites. Maleic acid and 3-aminopropyltriethoxysilane were used as precursors to make carbon dots and silica-protecting layers, respectively. It was observed that the presence of Si–O, Si–C, and Si–N protective layers suppressed the agglomeration of the neighboring CDs which resulted in a higher quantum yield. For example, by varying the ratio of the precursors green, yellow, and orange emission Si/CDs composites were obtained and their quantum yields were 34.06%, 38.07%, and 20.37%, respectively [61].

Table 1 presents some of the recent CD/support composites/hybrids that have been made using various starting reagents and synthesis methods, and also shows their potential applications. In summary, in most instances, the synthesized CDs have been observed to have similar optical transitions ($\pi - \pi^*$ and $n - \pi^*$) when analyzed using UV–vis, or similar G (graphitic) and D (defects) Raman bands [33,62]. In addition, the CDs have been observed to contain typical multi-functional groups such as C═C, C═O, C–O, COO^-/H, O–H, C–H, and N–H (when a nitrogen precursor is used) from FTIR spectroscopy, while the XRD data mostly reveal a (002) carbon diffraction peak with similarities to that of graphite [63].

In the subsequent sections, we now discuss the promising CD/support nanocomposites that have been made from various starting reagents, synthesis methods, and the properties of the composites with emphasis focused on how the physiochemical properties of the supported CDs give merit for their applications in a multitude of scientific fields.

5.2. SiO_2 support

CD-SiO_2 nanocomposites: The synthesis, embedment, and encapsulation of CDs on/in a silica matrix has received significant attention as compared to studies on other supports. This attention is due to the advantageous properties associated with SiO_2 supports, such as its structural morphology, large surface area, high loading capacity (especially hollow mesoporous silicas), and the ability of silica to homogeneously disperse CDs on its surface. CDs supported on SiO_2 have been found to overcome disadvantages such as the formation of CD aggregates, reducing aggregate-induced emission or fluorescence self-quenching, and by doing so they enhance their PL emission and quantum yields [78,79]. A study by Guo et al. demonstrated a facile approach to embed blue-emitting CDs into a mesoporous SiO_2 matrix. The embedded CDs exhibited an excitation-independent blue emission, as most CDs show an excitation-dependant nature. For example, excitation with different wavelengths (330 nm–390 nm) resulted in CDs emitting at the same wavelength; this was attributed to the CDs having uniform particle sizes and surface states. In addition, the nanocomposite that was modified by refluxing in the solvent exhibited a different life time decay suggesting that the fluorescent emissions were greatly influenced by surface states [80]. He and Rao monitored the fluorescent emission of CDs supported on SiO_2 nanoparticles for probing the presence of vanadium and copper, respectively. The nanocomposites (CD/SiO_2) were used as a nanosensor which exhibited outstanding fluorescent quenching in the presence of the metal ions that was attributed to a catalytic oxidation reaction occurring between the supported CDs and the metal ions. In addition, these nanocomposites exhibited good selectivity, high sensitivity, and these suggested a wide linear response range [81,82]. However, there was no detailed discussion about the nature interaction between CDs and the supports. Suggesting that there was no formation of covalent bonds between this CDs and the support but interfacial interaction was possible and resulted in altered optical emission in CDs.

Fig. 4 shows a schematic approach for coating CDs with a SiO_2 matrix. This synthesis procedure generated a SiO_2 support matrix which served as a support and a protection layer against environmental changes while the CDs maintained their luminescence properties. The CD@SiO_2 nanocomposites exhibited excellent emission properties under UV irradiation and the nanocomposites remained photostable due to the silica coating which protected the CDs from luminescent quenching. When compared to a commercial fluorescein sodium dye that was quenched after 65 min of UV illumination, the CD@SiO_2 nanocomposites PL emission was reduced by less than 20% after 65 min. The presence of the hydroxyl groups on the surface of CDs played a major role in initiating the gelation process of tetraethylorthosilicate. In addition, the hydroxy groups generated the formation of Si–O-CDs linkage which suppressed the aggregation of adjacent CDs. Furthermore, the gelatin silica served as a protective layer that induced the photostability and higher quantum yield of the nanocomposites [19].

Depositing CDs onto the surface of a support requires a solution medium that can facilitate the homogeneous distribution of the nanoparticles, by suppressing the aggregation or agglomeration of the CDs. Following the Derjagin-Landau-Verwey-Overbeek theory, Eurov demonstrated a procedure for depositing CDs on the surface of spherical silica particles. In this process, HCl, ammonia, and glycerol were used as a solvent mixture and this facilitated the deposition of CDs. The CDs were bound onto spherical silica matrices through the coagulation process in the solvent mixture. Although the nature of bonding between CDs and the support matrix was not discussed, it is worth noting that a change in particle diameter of the support matrix was influential on the PL emission and caused a redshift [83]. This route has also been used for the deposition of nitrogen-doped-CDs (N-CDs) on the surface of silica spheres, as well as on hollow and solid carbon spheres. A solution mixture comprising ethanol, ammonia, and water facilitated the homogeneous distribution of CDs on the surfaces of the supports. It was concluded that the nature of support can greatly influence the optical properties of the CDs due to the nature of the interaction between the two components. In addition, the CDs supported on a SiO_2 matrix exhibited intense fluorescent emission and a higher quantum yield [40].

Table 1
Summary of recent starting reagents, synthesis method, properties, observations, and applications of carbon-dots/support nanocomposites.

No	Starting reagent/s	Synthesis method	Composites	CDs particle size	Observations/Findings	Application	Ref
1	PEG 4000, citric acid, Urea and $CuCl_2{\cdot}_2H_2O$	Solvothermal	BC/ QPCuRC@$MSiO_2$@PDA	10.43 nm	Excitation wavelength-dependent PL emission, with maximum PL emission @ 722 nm (Ext. 360 nm). Improved antibacterial activity, biocompatibility and multifunctional synergistic effect.	Wound healing and bioimaging	[64]
2	Citric acid and Urea	Microwave-assisted	dU6-CD/Eu	0.99 ± 0.3	Excitation wavelength-dependent PL emission, maximum emission @ 475 and 530 nm (Ext. 380 and 395 nm). Efficient and tunable white light emission, energy efficiency.	WLED prototype design	[65]
3	*Ginkgo biloba* leaves	Hydrothermal	HF-CDs	4.2 nm	Good sensitivity and selectivity, with a good limit of detection.	Trace detection of herbicides residues	[66]
4	Chitosan	Solvothermal	N-CD/TiO_2	2–8 nm	Synergistic effect between CDS and TiO_2. Excitation wavelength dependent, enhanced photosensitivity toward visible light, prolonged photogenerated charge carrier lifetime, suppressed non-radiative decays.	Photoelectrochemical water oxidation activity,	[67]
5	Coal samples	Ammonia hydrothermal cutting	N-CD/Cu NRs	5 nm	Reduction of the band gap, higher generation of radicals, and charge carrier transferability of the composite. Enhanced photodegradation of aldehydes, phenols, acids, amines, alkanes, ketones, and ethers pulp liquor and subsequence H_2 production.	Photoecletrocatalytic degradation of cotton black pulp liquor and H_2 production	[68]
6	Citric acid and ethylenediamine	Hydrothermal	CD/g-C_3N_4	2 nm	Higher sensitivity and extraction of chlorobenzenes owing to abundant active sites from CDs. Increased surface area and good reproducibility.	Solid phase micro-extraction of chlorobenzenes	[69]
7	Amino acid (Tryptophan)	Hydrothermal	$Pt_1Pd_1Sn_1$/CNT-NCD	6.5 nm	Higher catalytic activity and stability for electro-oxidation, improved surface area, NCD surface states facilitated $-CO_{ad}$ oxidation.	Methyl formate and dimethyl ether electro-oxidation	[70]
8	Graphite rods	Electrolytic	TiO2/N-CD/Au		Enhanced photocurrent density and separation of electron-hole pairs, higher laser response. Synergistic effect between N-CD and Au.	Photoelectrochemical water splitting	[71]
9	Cetylpyridinium chloride	Microwave	Ludox@CD	3.59 ± 0.02 nm	Yellow fluorescent emission @545 nm when excited using @380 nm wavelength, good quantum yield (QY 34%), Improved latent fingermark imaging, nanocomposite exhibited anticancer activity for MCF-7 breast cancer cell lines, low toxicity, and biocompatible. A higher concentration of Ludox support matric could suppress the emission of CDs.	Latent fingerprint detection and biomedical applications	[72]
10	Glucose and urea	Oil bath/heated copra oil	ZnO/CD	2–5 nm	Excitation wavelength dependency of CDs, Enhanced photodegradation of methylene blue under visible light. Enhanced photocurrent response. Suppressed electron-hole recombinations and extended visible light response.	Photocatalytic degradation of methylene blue	[73]
11	Citric acid and ethylenediamine	Hydrothermal	Au@Ag@CD	4.5 nm	Synergetic catalytic oxidation of 4-CN, Reduction in photocurrent response (capture the irradiating light and electron donors of the photoelectrochemical biosensor system), energy transfer, higher sensitive detection and selectivity of microRNA-155, promise for application as biomarker and disease diagnosis.	Photoelectrochemical biosensing of microRNA	[74]
12	Graphite rods and ammonia	Electrolysis and hydrothermal post-N-modification with ammonia	TiO_2/N-CD	2–8 nm	CDs induced electron-trap effect. Enhanced photogenerated charge separation. Improved conductivity and charge carrier transfer, N-CDs enhanced photoelectrochemical performance, Enhanced photocurrent	Photoelectrochemical water splitting (composite served as a photoanode)	[75]

(*continued on next page*)

Table 1 (*continued*)

No	Starting reagent/s	Synthesis method	Composites	CDs particle size	Observations/Findings	Application	Ref
					response, decreased on-set potential, and suppressed electron-hole recombinations.		
13	Ethylene glycol (EG), ethanolamine (EA), ethylenediamine (ED) (All in Hydrogen peroxide)	Polyol process	CD (ED)/CNT	1.95 ± 0.32 nm	Scalable synthesis, uniform particle sizes, excitation wavelength dependent with maximum PL emission @467 nm at excitation @320 nm, higher PL emission owing to N content, CD (ED)/CNT composite exhibited inferior catalytic activity with enhanced oxygen reduction reaction compared to Pt/C, hybrid showed better durability and methanol tolerance than commercial Pt/C electrode, fast electron transfer rate, and excellent electrocatalytic activity.	Oxygen reduction reaction in fuel cells	[76]
14	Lignin and ethylenediamine	Hydrothermal	Pt-CD@CdS	1.5–2.8 nm (Av. 2.16 nm)	N-CDs were used as a Pt support matrix to curb agglomeration of Pt particles, composite showed higher photostability, the synergistic effect of Pt, CD, and CdS with enhanced separation, transport, and the reaction of charge carrier, anchoring of single Pt atom via N, C, and O interactions, enhanced H_2 evolution by the composite due to enhanced interface transfer of charge carrier generated in CdS, enhanced visible light absorption. Faster transient photocurrent response, suppressed PL emission of the composite owing to efficient photogenerated charge carrier separation. PL emission between 500 and 700 nm when Excited with 380 nm wavelength.	Photocatalytic H_2 evolution reaction	[77]

When agglomeration was suppressed the intensity of the photoluminescence emission in the CDs was enhanced, self-quenching of the PL emission was reduced, and a higher QY was obtained.

In another study, the mobilization of N-CDs on the surface of porous SiO_2 spheres was achieved by making use of deep eutectic solvents as a disposable agent for achieving a homogeneous distribution of CDs on the surface of silica spheres (Fig. 5). The SiO_2-CD nanocomposite was used as a stationary phase in a liquid chromatography column and the incorporation of CDs proved to be feasible for use as an adsorbent for use in liquid chromatography. The SiO_2-CD nanocomposite was used as a stationary phase for a *Cordyceps* sample and exhibited a selectivity toward polar compounds with good separation and detection of uridine and inosine [84]. CDs have been infiltrated within a porous SiO_2 structure, followed by pyrolysis, which resulted in the formation of a SiO_2/CD nanocomposite with the CDs being entrapped within the SiO_2 pores. The embedded CDs showed fluorescent emissions. The embedded CDs exhibited an enhanced sensitivity for trypsin and adenosine triphosphate. The bimodal detection of the fluorescent emission of the embedded CDs was reduced and completely quenched as the concentration of these analytes was increased. In addition, the embedded CDs exhibited different fluorescent emissions (blue-shifted) as compared to CDs in the solution state; this was attributed to the different surface states that existed between the embedded solid CDs and CDs in the solution. Furthermore, the CDs that were synthesized in the pore matrices of silica were smaller in size as compared to CDs that were produced from solution. Therefore, it was suggested that the particle sizes and the surface states of the CDs were influential in generating the PL emissions of the CDs [85].

The photoluminescence emission of the CDs was quantified by calculating the quantum yield (QY). A silane-functionalized CD (CD/SiO_2) nanocomposite with a high surface area was synthesized using TEOS and CTAB and this was reported to have a QY of 47%. The QY could also be enhanced by the incorporation of Ag nanoparticles onto the CD/SiO_2 nanocomposites. The enhancement of the PL emission of the CD/SiO_2 by Ag nanoparticles was attributed to an increase in the O binding energy which induced a local electromagnetic field and a plasmon coupling effect [86]. Pyrolysis of rice husk to make CDs gave a meso-SiO_2/CD nanocomposite with a promising potential for use in labeling yeast cells (Fig. 6). The nanocomposites exhibited good biocompatibility, nontoxicity to Vero cells, high drug loading, and were easy to synthesize. The enhanced photoluminescence emission made it valuable for *in vitro* bioimaging of yeast cells [87]. The study has demonstrated the simple and facile method for embedding CDs within the pore matrix of mesoporous silica. However, no detailed mechanism explained how the interaction between CDs and the support influenced the PL emission. It can be suggested that the synthesis procedure used in this study were simplify the purification processes that are employed after CDs synthesis since the CDs get entrapped within the pore matrix.

Eurov et al. demonstrated a method for the fabrication of different CDs onto a nano-porous silicate glass (NSG) (Fig. 7). Two types of CDs, namely, CD-1 and CD-2 were prepared using a combination of citric acid and ethylenediamine, and urea, respectively. The FTIR spectrum of CD-1 and CD-2 suggested that the CDs contained mostly secondary and primary amide functional groups, respectively. Interestingly, the CDs that were in solution and the solid state (on the NSG) were observed to have different photoluminescence emission profiles. As shown in Fig. 8, the optical properties of CDs dispersed in solution and a CD/NSG (solid) nanocomposite exhibited different absorption characteristics under UV–vis irradiation. Their photoluminescence mapping varied depending on the type of functionalities (chromophores) present within the CDs. Interestingly, the CD-2/support showed an increased QY (from 17% to 40%) while for the CD-1/NSG the QY did not change significantly. This

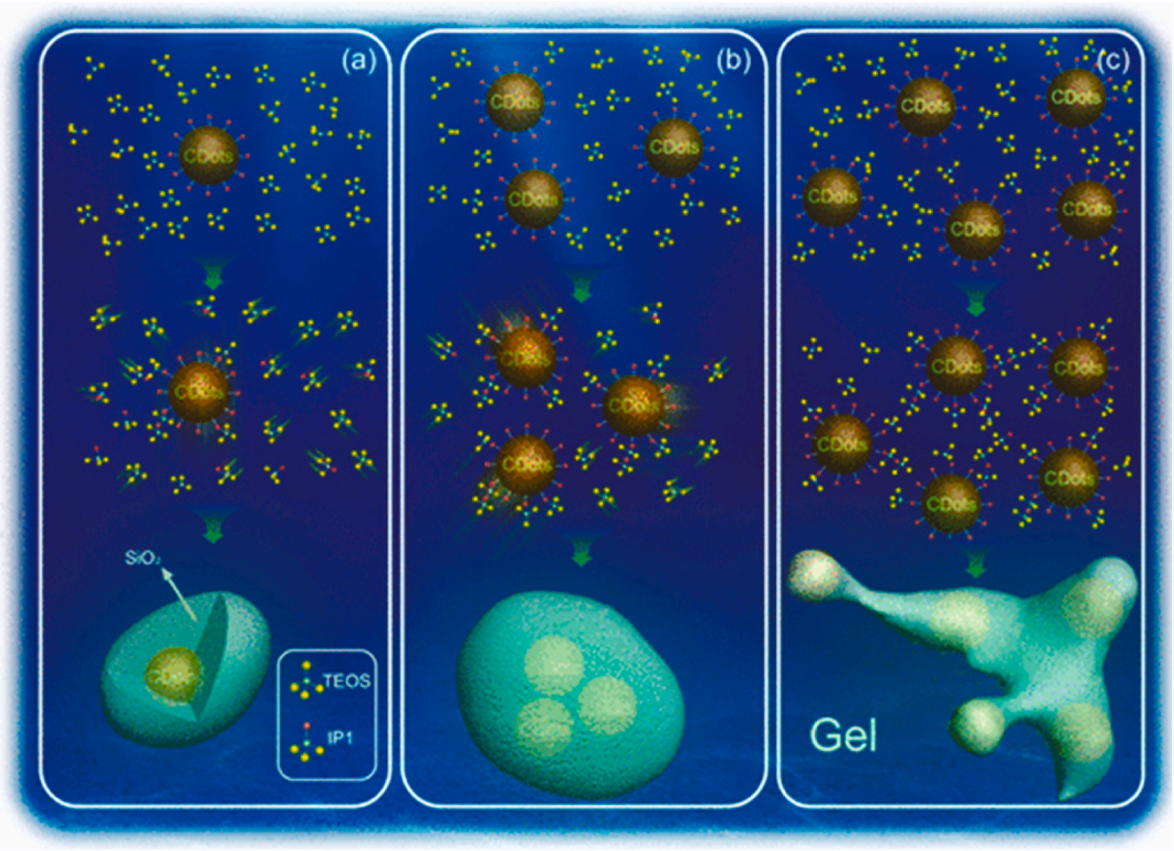

Fig. 4. Schematic of the formation of a CD@SiO_2 composite nanoparticles/gel at (a) low, (b) medium, and (c) high concentrations of CDs in ethanol solution. Adapted from Zhou et al., (Adapted with permission from American Chemical Society, copyright 2017) [19].

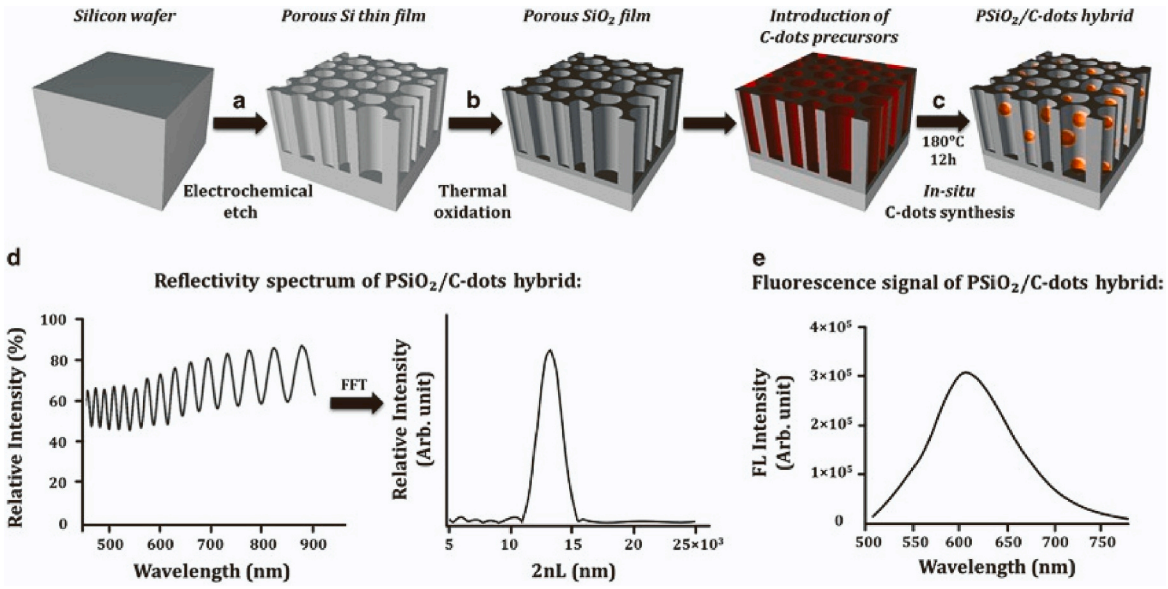

Fig. 5. Construction of the CD/$PSiO_2$ hybrid ($PSiO_2$, porous silicon oxide) and the two sensing modalities. (a) Anodic electrochemical etching was used to prepare a $PSiO_2$ layer from a single-crystal Si wafer; (b) the freshly etched sample was thermally oxidized at 800 °C; (c) the carbonaceous precursor was incorporated in the $PSiO_2$ pores for the in situ synthesis of the CDs. Subsequent water evaporation and slow heating result in the formation of CDs. (d) Optical reflectivity and (e) fluorescence emission were generated simultaneously in the CD/$PSiO_2$ hybrid, (Adopted with permission from Springer Nature, copyright 2018) [85].

indicated that the photoluminescence emission of the CDs was not reduced or quenched when embedded in the NSG [88]. These observations further suggest that embedding of CDs onto NSG did not lead to nonradiative combination, a common drawback for supported CDs or when the CDs are measured in the solid state.

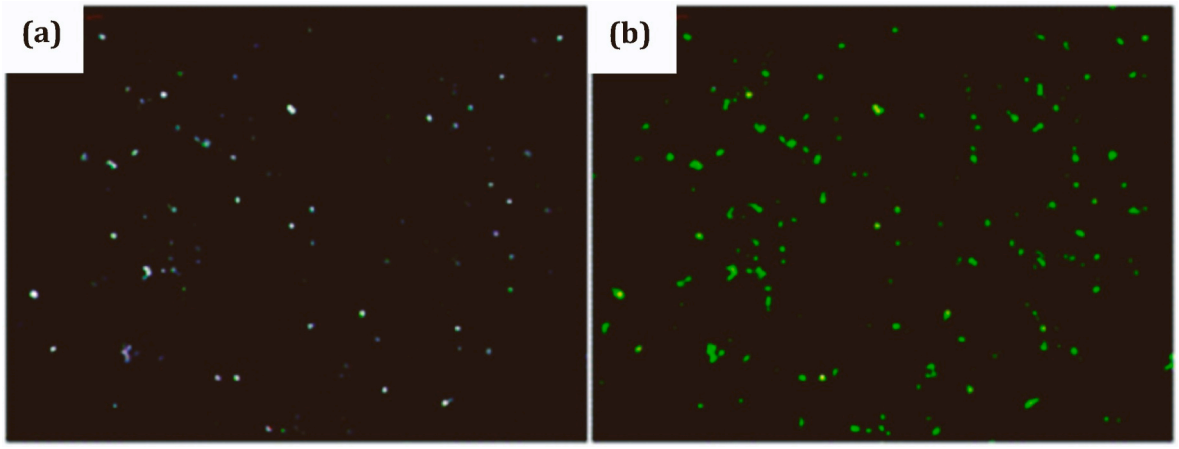

Fig. 6. In vitro visualization of yeast cells using meso-SiO_2/CD nanocomposites, (a) white light (b) fluorescent illumination, (Adopted with permission from Royal Society of Chemistry publishing, copyright 2011) [87].

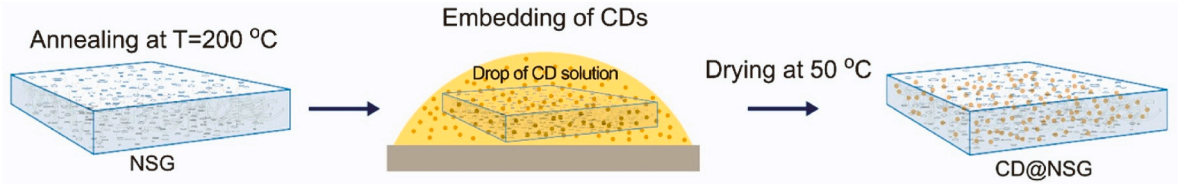

Fig. 7. Schematic representation of CDs embedded onto the nanoporous silicate glass, (Adopted with permission from Nanomaterials (MDPI), Basel, Switzerland, copyright 2011) [88].

5.3. Zeolites and MOFs

Zeolites are naturally occurring crystalline, hydrated aluminosilicates of alkali and alkali earth cations. Their well-defined pore structure is useful for the embedment or incorporation of CDs. As shown in Fig. 9 (a), a metal-organic framework, namely zeolite ZIF-8, was synthesized and used as a support matrix for CDs and Au nanoparticles. The presence of CDs was reported to affect the size of the nanocomposite and the CDs/ZIF-8 exhibited coordination interaction between Zn^{2+} ions of the MOF and the terminal carboxyl or/and N-groups of the CDs. The zeolite support matrix not only acted as a CD carrier but was found to lead to a 6-fold enhancement in the electrochemiluminescence emission signal of the supported CDs as compared to bare CDs. The enhancement of the signal was attributed to the pore structure of the ZIF-8 and the mechanistic ability to convert CDs to negative charge CDs in $K_2S_2O_8$ medium. The presence of Au nanoparticles further induced a further 7-fold increase the intensity when compared to the bare CDs. The CD/ZIF-8/AuNPs samples were used as an electrochemiluminescence emitter for monitoring cell apoptosis. In the study, the presence of CDs in the nanocomposite allowed for the quantitative monitoring of the Caspase-3 activity during cell apoptosis and showed a linear response for detection (with good sensitivity and stability) of Caspase-3 with a limit of detection of 0.03 pg/mL (Fig. 9 (b)). The nanocomposites demonstrated a potential for use as a biosensor for screening novel small molecule inhibitors acting as therapeutic agents [89].

In another study, a metal-organic framework (MOF) based sensor embedded with CDs and a molecularly imprinted polymer was developed for use in monitoring quercetin. As shown in Fig. 10, the fluorescence emission from the nanocomposites (CDs/MOF/MIP) was monitored as a function of increasing quercetin concentration. It was observed that as the concentration of the analyte was increased the CDs fluorescence response was decreased and could be quenched (fluorescence quenching). This nanocomposite showed higher selectivity and sensitivity toward quercetin when tested against isorhamnetin, epicatechin, daidzein, and rutin. Interestingly, the synergistic selectivity of the CDs and MIP exhibited good selectivity towards quercetin extracted from commercially available Ginkgo biloba capsules. The presence of CDs in the nanocomposite exhibited good selectivity of the quercetin [90]. Further fabrication of CDs on various MOFs such as ferrisilicates (NaFZ) and imidazolate (ZIF-8) to give N-CDs@NaFZ and N-CDs/R-CDs@ZIF-8 was achieved, and the nanocomposites were used for sensing Hg^{2+} in fish [91], and also Pb^{2+} [92], and bisphenol [93], in wastewater [94]. A poor response was observed for metal ions such as Fe^{2+}, Fe^{3+}, Na^{2+}, Cu^{2+}, K^{+}, Mg^{2+}, Ba^{2+}, Ba^{2+}, Cd^{2+}, Mn^{2+}, Zn^{2+}, Ag^{2+}, Ni^{2+}, Co^{2+}, and Cu^{2+} [91]. Another similar composite AuNPs-ErCDs-MOF (Er = electron reduced) showed good selectivity (monitored by the peak current on a modified GCE) when compared with inorganic ions such as K^{+}, Mg^{2+}, NO_3^{-}, Na^{2+}, $Zn^{2+,}$ and Cl^{-} [93]. The embedding of CDs on the pore architecture of the MOF has been presumed to result in the formation of strong hydrogen bonding and/or covalent bonding between the two components. Interestingly, the quenching of the fluorescence emission was attributed to excited state electron transfer from the donor nanocomposite to the metal ions of interest. For example, in Hg^{2+} ions the excited electrons were transferred from the nanocomposite (-OH and –COOH of the CDs) to the empty d orbitals of Hg^{2+} ions resulted in the formation of coordination bonds and complexes [91]. In addition, it was proposed that the mechanism of action that resulted in the quenching of the fluorescent emission in CDs was due to the formation of the coordination bond between CDs and Pb^{2+} ions. Upon the addition of Pb^{2+} ions, it was observed that the morphology of the CDs/ZIF-8 nanocomposite collapsed. The collapse in the morphology can be attributed to the formation of the coordination bonds and complexes between the N-groups in CDs and the Pb^{2+} ions. This was further confirmed by XRD, UV–Vis, and FTIR. Therefore, upon the addition of Pb^{2+} ions, the N-groups of the CDs strongly interacted with Pb^{2+} ions and this resulted in the structural collapse of the ZIF-8 [92]. The enhanced sensitivity and selectivity of the CD-MOF-based nanocomposites have widened the application spectrum for nanocomposites applications and fabrication in sensing devices.

A study by Xu et al. has demonstrated the use of CDs as a saturable

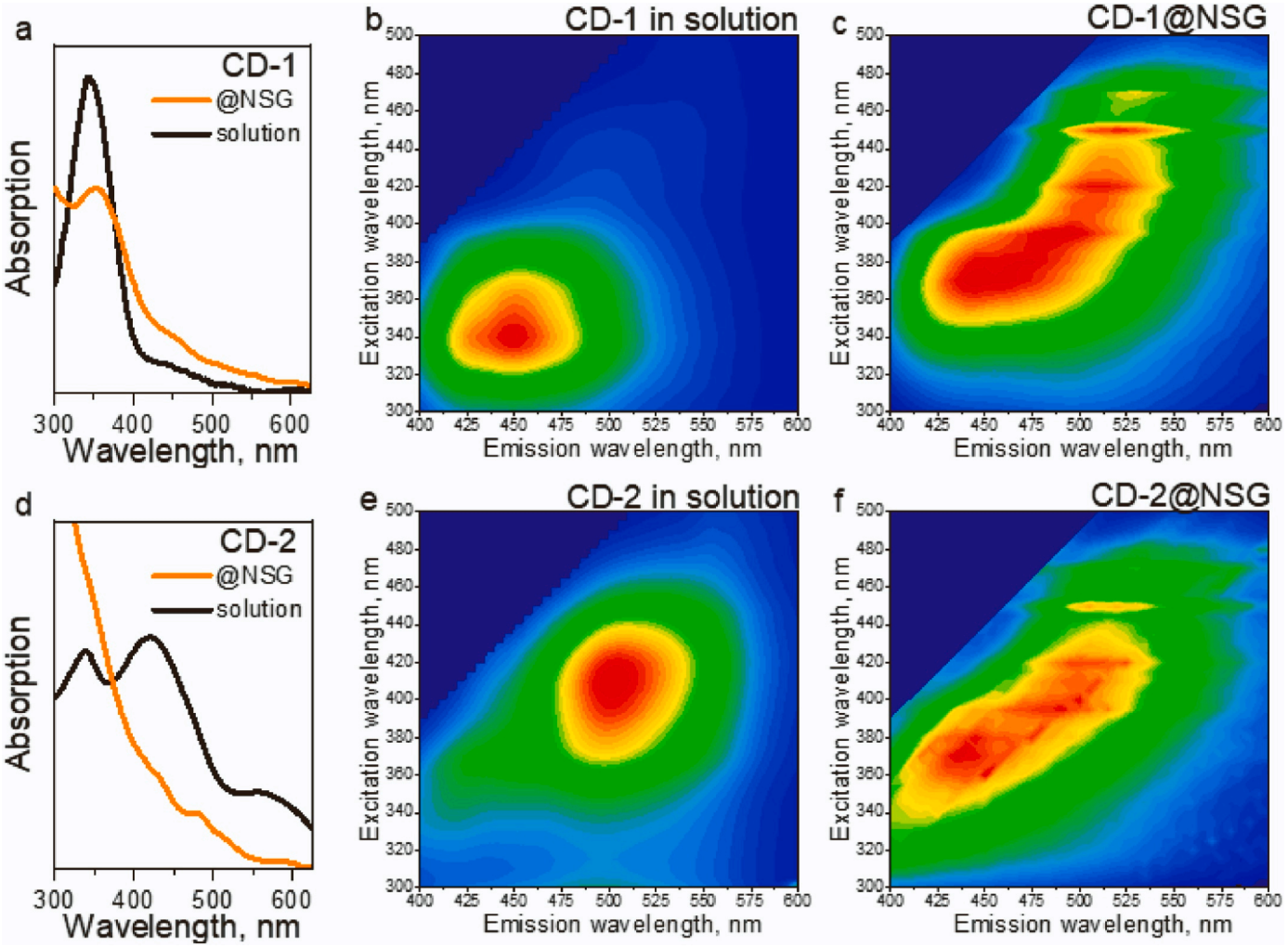

Fig. 8. (a,d) Absorption spectra of CDs in solution (black) and CD/NSG (yellow), (b,e) photoluminescence maps of CDs in solution and (c,f) CD/NSG nanocomposites, (Adopted with permission from Nanomaterials (MDPI), Basel, Switzerland, copyright 2011) [88].

absorber to generate a Q-switched yttrium-doped fiber laser. As shown in Fig. 11, the CDs were fabricated in the pore channels of zeolite SAPO-46 (AFS). The saturation intensity of CDs/AFS nanocomposite was found to be 8.5% and 10.1 $MWcm^{-2}$, respectively. The nanocomposite could be used as a saturable absorber for short-pulsed laser generation. In the study, it was observed that integrating the CD/AFS nanocomposite into the yttrium-doped fiber laser gave improved stability of the pulsed fiber laser, and the ease of handling the photonic device allowed operation at a high pump power [95]. The use of CDs in this field is still limited and fundamental literature that discusses the mechanistic insight on how CDs enhanced the desired properties is essential.

5.4. Carbon supports

Carbon is one of the most common elements that have been explored as a support for many elements/molecules/materials [96]. Carbon can form strong carbon-carbon bonds giving rise to various oligomers and polymers with numerous dimensions leading to the formation of many different structures [97,98]. The differently structured carbon materials that have been used as a support matrix for CDs are described below.

CD/chitosan nanocomposites: Chitosan (Chn) is a highly available biopolymer that is abundant and occurs naturally in the shells of arthropods such as crabs, shrimps, and lobsters; chitosan is regarded as a cheap and environmentally friendly material [99,100]. Structurally, Chn is formed by the alkaline deacetylation of chitin and it is a linear copolymer of D-glucosamine and N-acetyl-D-glucosamine [101]. It has been used as a precursor for the synthesis of nitrogen-doped CDs and as a support matrix. Huang et al. synthesized CDs from a mixture of polyethylene glycol-200 (PEG-200) and glucose under microwave irradiation. The obtained CDs were supported on Chn to form a CD/Chn nanocomposite using vigorous ultrasonication. The CD/Chn was used in the electrochemical detection of dopamine. The CD/Chn nanocomposite was deposited onto a glass carbon electrode surface. It was observed that the presence of the CDs enhanced the conductivity and sensitivity of the nanocomposite, which resulted in a better electrochemical response for dopamine detection than that obtained from the bare GCE. In addition, the enhanced electrochemical response was attributed to the carboxylic groups (negatively charged surface) which favored an electrostatic interaction with the dopamine analyte [102]. In biological endeavors, Omidi and co-workers demonstrated the use of a CD/Chn nanocomposite for wound dressing in rats. It was reported that the nanocomposite was biocompatible, nontoxic, and exhibited better effective antibacterial properties as compared to chitosan or CDs alone. As shown in Fig. 12, the CD/Chn nanocomposites exhibited good pH sensing and antibacterial properties when used as a wound-dressing nano-agent. After 18 days the wound was completely healed when a CD/Chn nanocomposite was used (while a control or bare chitosan did not heal the wound completely) and this was attributed to a synergistic effect of the Chn and CDs [103].

Fig. 13 shows a stepwise procedure for the preparation of a CD/Chn

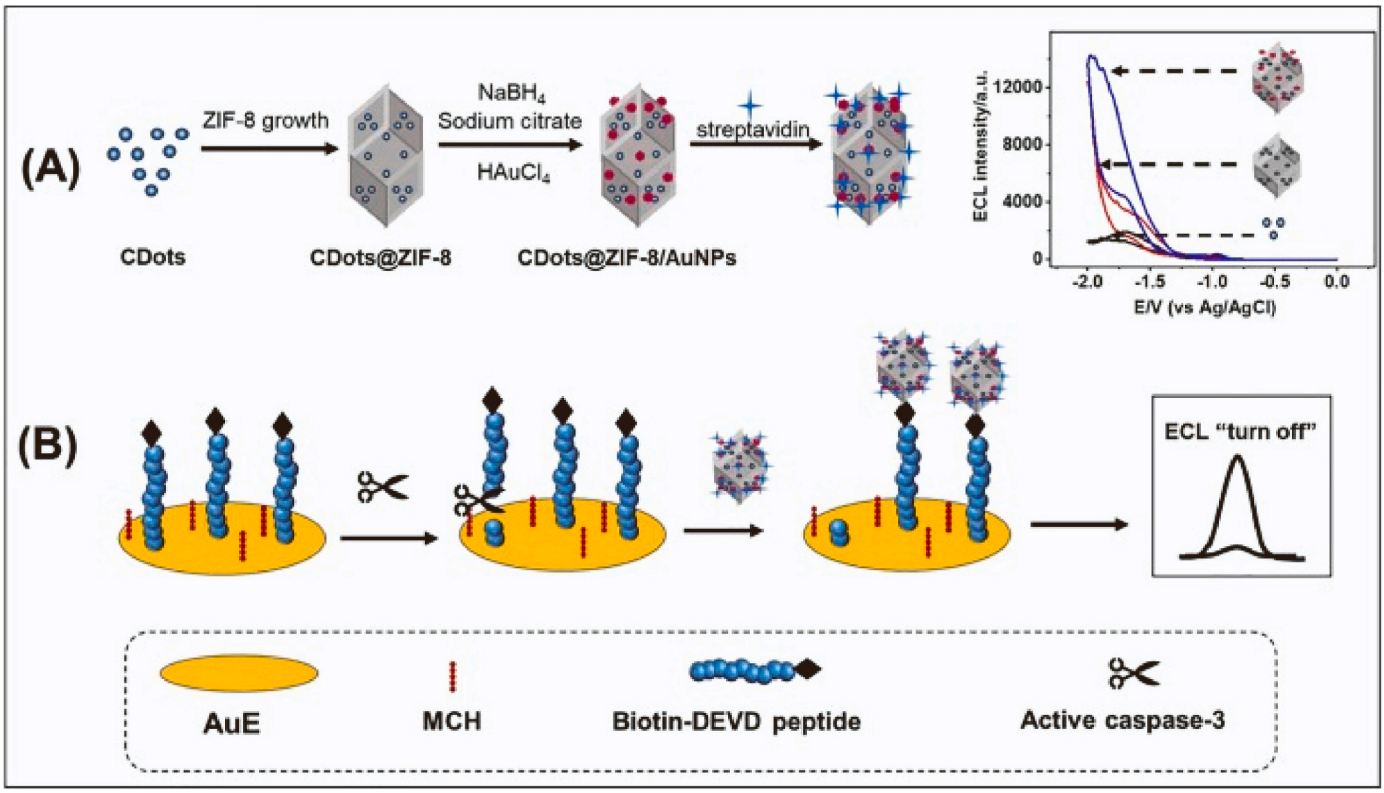

Fig. 9. (a) Schematic representation of CD/ZIF-8/AuNPs-SA fabrication, (b) sensing of caspase-3 using CD/ZIF-8/AuNPs nanocomposite as an electrochemiluminescence reagent, (Adopted with permission from Elsevier B.V, copyright 2021) [89].

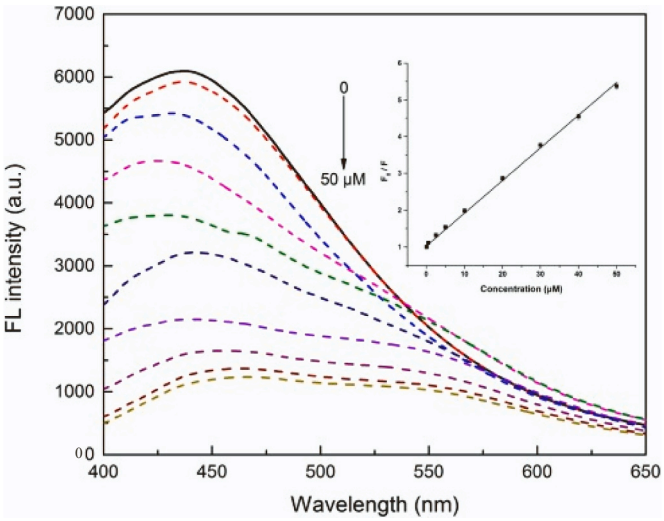

Fig. 10. Fluorescence response of CD@MOF@MIP nanocomposite towards increasing concentrations of quercetin, (Adopted with permission from Elsevier B.V, copyright 2019) [90].

nanocomposite film. The presence of CDs on a CD/Chn nanocomposite hydrogel exhibited enhanced UV–vis blocking, increased tensile strength, good thermal stability, and a good swelling ratio. The UV–vis blocking resulted in a decreased HOMO-LUMO energy gap which caused a bathochromic shift toward the visible region. The tensile strength increased from 5.1 MPa to 18.6 MPa for CDs and the CD/Chn nanocomposite hydrogel, respectively. In addition, the thermal stability was increased by up to 100 °C, while the swelling ratio was increased from 52.2% to 82.2% for the bare CDs and the CD/Chn nanocomposite hydrogel, respectively. The enhancement of the above-mentioned properties and reduced energy gap was attributed to the strong electrostatic interaction between the CDs and Chn. The strong electrostatic interaction through hydrogen bonding was made possible by the presence of positively charged NH_3^+ groups on Chn and the negatively charged surface of the CDs. This led to the realization of hydrogen bonding between NH_3^+ and/or -CH_2OH of Chn and the –OH groups of CDs. In addition, the conjugated aromatic structure of the CDs also plays a pivotal role in the enhancement of the properties of CDs/Chn nanocomposites [104]. These properties make the CD/Chn nanocomposite hydrogel a promising nanostructured material for use in biomedical imaging and other industrial applications.

CDs/starch phosphors nanocomposites: The superior properties of CDs will without doubt find practical application in many fields. In the law enforcement area, Dong et al. demonstrated the used of red fluorescent CDs supported on starch for accurate identification of latent fingerprints on various substates. In their study, they used a mixture of citric acid, p-phenylenediamine, and phytic acid in formamide via the hydrothermal method in an autoclave reactor for the synthesis of red fluorescent CDs. Thereafter, the nanocomposite (CDs/starch) was designed by mixing the two components in ethanol and stirring them for 24 h (Fig. 14). Fig. 15 shows the photographs of the latent fingerprints that were collected. Due to the presence of CDs in the nanocomposite, it was possible to use the powder dusting method to identify and visualize the latent fingerprints owing to the red fluorescent properties of CDs. When the nanocomposite was compared to powder CDs, the powder CD's fluorescent intensity was reduced due to the formation of aggregates that resulted in molecular orbital overlapp of the neighboring CDs. However, when CDs were supported on starch (1:40 ratio) their fluorescent emission was retained owing to homogeneous distribution which suppressed the formation of aggregation. The strong interaction between CDs and starch resulted in a blueshift in the absorption spectrum of the composites to 550 nm as compared to 570 nm for the pristine CDs. Furthermore, the CDs/starch nanocomposite had a high

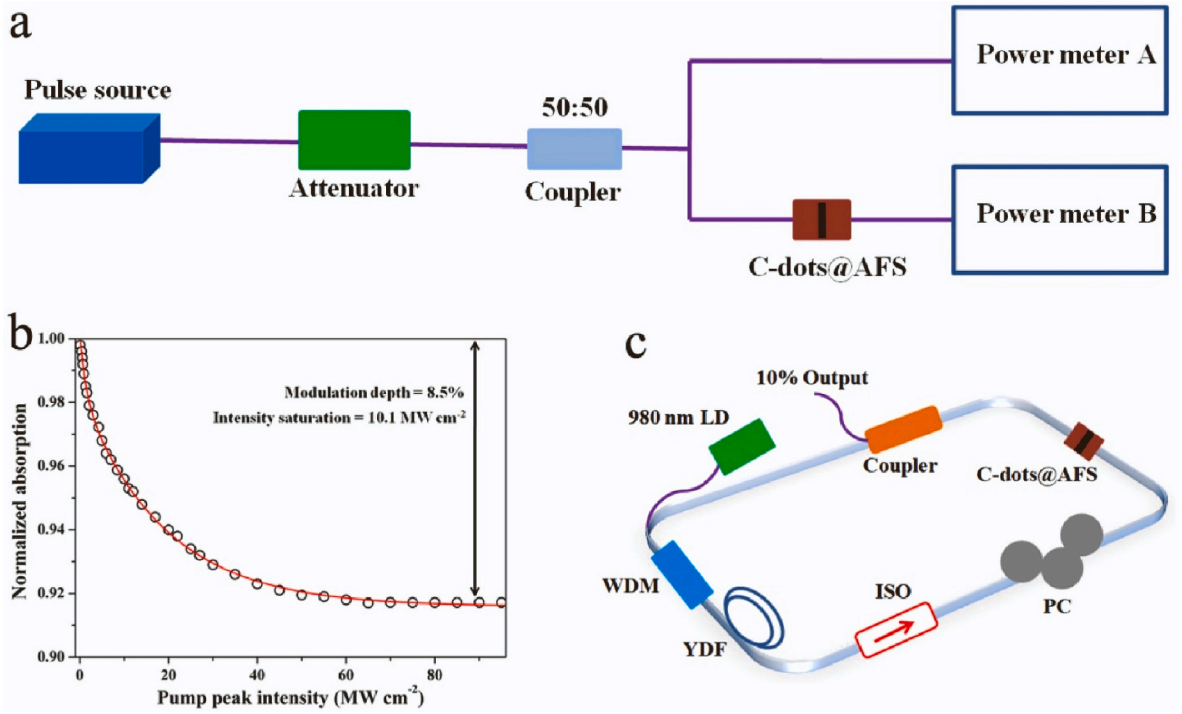

Fig. 11. (a) The setup of a balanced twin-detector measurement. (b) The normalized absorption of the CD/AFS saturable absorber as a function of pump pulse peak intensity. Dots: measured data; red line: fitting to the data. (c) A schematic diagram of the ytterbium-doped fiber laser, (Adapted with permission from Elsevier B.V, copyright 2018) [95].

photoluminescent quantum yield (21%) [105].

CD/carbon nanotubes nanocomposites: In the early 1990s, studies by Iijima on carbon nanotubes (CNTs) provided the impetus for the synthesis and understanding of CNTs [106]. CNTs have a high surface area, good mechanical and chemical stability, good thermal conductivity, and are easy to functionalize. Supporting CDs on the surface of CNTs has led to the synthesis of composites that have been used in photocatalysis, electrochemistry, adsorption studies, etc. In adsorption studies, CDs have been supported onto magnetite-modified magnetic carbon nanotubes. The nanocomposite exhibited excellent carbamazepine removal and reached up to 80% removal within 3 h. The composites were also effective for the removal and inhibition of E. Coli microorganisms. The removal of carbamazepine and inhibition of E. Coli was attributed to the presence of CDs on the composites due to the presence of carboxyl functional groups [107].

The fabrication and practical application of metal-free catalysts have been a topic of interest to the science community. One of the first systems to be investigated was a nanocomposite made from boron/nitrogen carbon dots (BN-CDs). The material was synthesized via a hydrothermal method, using L-aspartic acid and boric acid as nitrogen and boron sources, respectively. The BN-CDs material was supported onto MWCNTs using both hydrothermal and pyrolysis methods. These BN-CDs/CNTs nanocomposites were used for the oxygen reduction reaction (ORR) using a three-electrode system. It was reported that the abundant mesopores and micropores facilitated a good diffusion of reaction species and favored an efficient electron transfer rate during the electrochemical reaction. The optimum BN-CDs:CNTs ratio that gave a good performance for ORR was 400 mg:150 mg. The nanocomposite was pyrolyzed at 800 °C for 4 h before use. The BN-CDs/CNTs nanocomposites showed good ORR performance and the obtained results from polarization curves were comparable to a Pt/C electrode. This result was attributed to the synergy of pyridinic N and the BC_3 content in the BN-CDs. In addition, the BN-CDs/CNTs nanocomposites exhibited a better current density (i.e. good cycle stability) of 76% than the Pt/C electrode (52%) after 10 h [108].

In many instances, *ex situ* synthesis methods have been used to support CDs onto the surface of CNTs. Li et al. demonstrated a pyrolysis method for the synthesis of very small CDs using MWCNTs as support. As shown in Fig. 16 and 2-(N-morpholino)-ethanesulfonic acid (MES) was supported on the surface of MWCNTs. Due to hydrogen bonding and π-π interactions, the MES precursor was uniformly dispersed on the surface of the MWCNTs. The MES was used as a CD precursor and MES/MWCNTs and MES were both pyrolyzed at 300 °C, for 2 h. Interestingly, the MWCNTs as a support matrix favored the synthesis of CDs with a uniform particle size of 0.69 ± 0.14 nm. The CDs prepared from MES alone had a 17.8% quantum yield while the CDs which were prepared using MWCNTs as support exhibited a higher quantum yield of 42.8% [109].

CDs@HCSs: Hollow carbon spheres (HCSs) have emerged as carbon support for minimizing the formation of a metal nanoparticle aggregates [21]. HCSs can serve as an encapsulating cage that confines molecules or metal nanoparticles in the HCS interior such that migration of large particles to the outside of the cage is minimized [21,110]. One interesting advantage of encapsulating nanoparticles inside HCSs is that the HCSs then serve as a nanoreactor and the nanoparticles inside the cavity are not lost during application (i.e. easy recovery and reusability of the nanoparticles). Chen et al. demonstrated a one-step in-situ method for the synthesis of CDs encapsulated inside HCS using fish scales and collagen as starting materials. The study offered a strategy for preparing fluorescent HCSs/CDs with a high QY (~38%) in a scalable route [111]. Another study by Lou et al. demonstrated a method for the encapsulation of carbon species inside carbon nitride hollow spheres. However, the luminescent emission intensity became weaker as the graphitic carbon content increased [112]. A remarkable study in which polymer dots were encapsulated inside of an HCS cavity was reported by Qiao and co-workers, Fig. 17. Here the QY of the entrapped CDs was lowered as compared to the untrapped CDs. Interestingly, the entrapment of CDs inside a porous matrix could simplify the purification and reusability of caron dots. As shown in Fig. 17, the core-shell procedure for the encapsulation of CDs inside HCSs follows three steps, (i) synthesis of

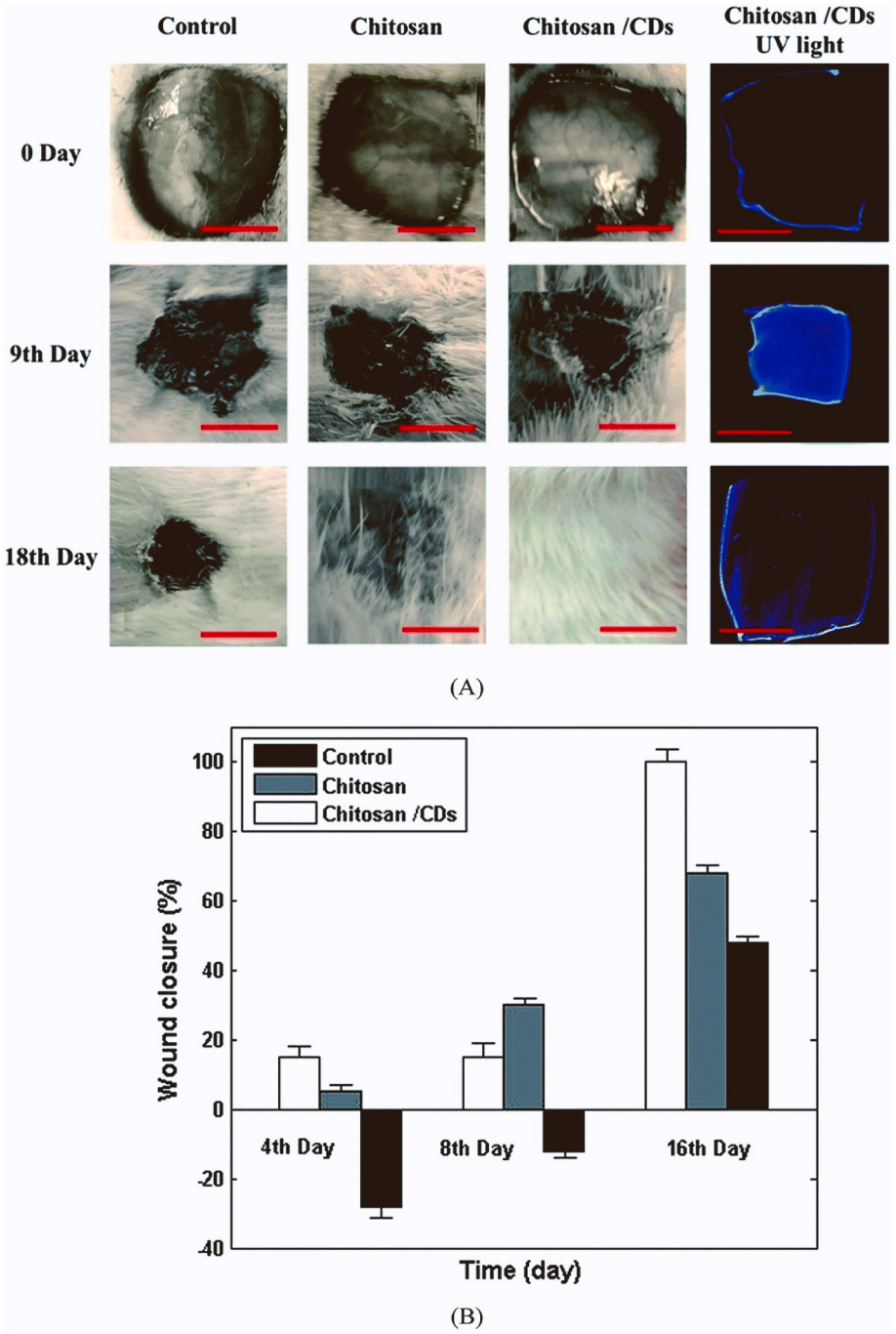

Fig. 12. (A) The visual images of the untreated (control) and treated wound with chitosan, and CD/chitosan nanocomposite at different stages (0, 9, and 18 days); the fluorescence images on the right-hand side show the pH sensitivity of the CD/Chn nanocomposite. (B) Wound closure percentage of untreated (control) and treated wounds (chitosan and CD/Chn nanocomposite), (Adopted with permission from Royal Society of Chemistry, copyright 2017) [103].

porous HCSs, (ii) infiltration of a CDs precursor inside the HCSs cavity, (iii) polymerization of the CDs precursor via reflux at 90 °C [110].

CD-polymer nanocomposites: Linear and nonlinear polymeric compounds are good candidates for facilitating the immobilization, embedment and stabilization of molecules, and nanoparticles. Since the discovery of CDs, polymeric networks such as polyethylene glycol (PEG), polyethylene, cytopore, and polystyrene have been used as support for CDs. These polymeric support matrices have shown solid-state photoluminescence emission for the nanocomposites. A multifunctional PEG-Chn/CD hybrid nanocomposite gel was synthesized and applied as a nano-agent for fluorescent imaging, pH response drug carrier delivery, and synergistic therapy. The presence of the CDs in the nanocomposites facilitated the realization of fluorescent pH sensing (i.e. a stable optical property), and cellular imaging, and enhanced the loading of anticancer drug molecules [113]. Gogoi and Karak supported carbon dots on polyurethane and used the composite for the solar-driven production of hydrogen peroxide [21]. The bandgap of the CDs facilitated the splitting of water and ethanol under solar irradiation. The composite was reported to be biodegradable using the *P. aeruginosa* microorganism [25]. Li et al. immobilized CDs on the microcarrier, cytopore, and used the composite for the rapid adsorption of cadmium which reached adsorption equilibrium within a minute and gave a maximum adsorption capacity of 2420 μg/g with good selectivity [114]. In other studies, Abbas and co-workers demonstrated a one-pot synthesis

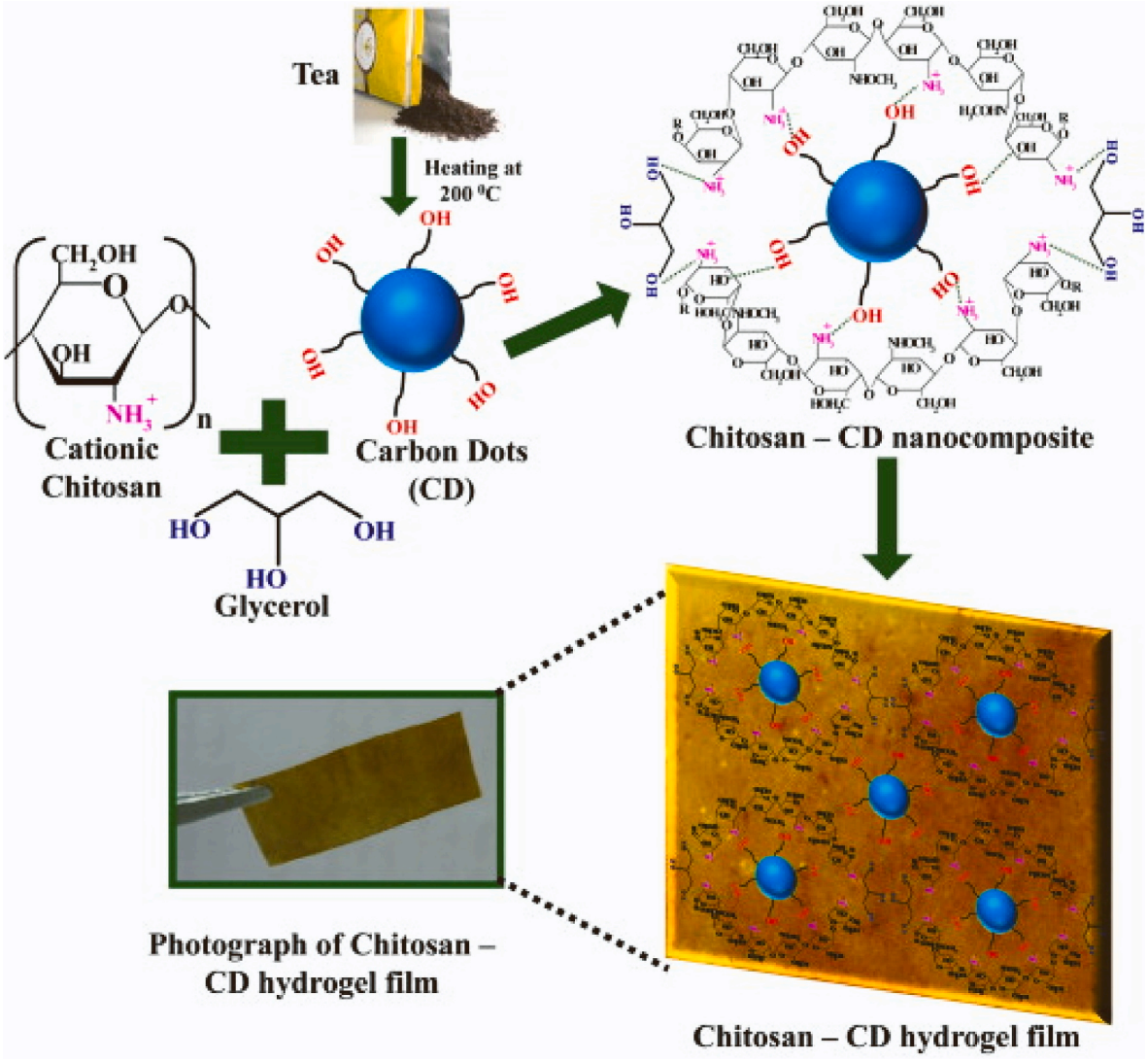

Fig. 13. The schematic procedure used for the preparation of chitosan-carbon dots nanocomposite film (Adapted with permission from Elsevier ltd, copyright 2014) [104].

to make multifunctional blue, green, and red-emitting CDs embedded in polymeric frameworks. As shown in Fig. 18, the embedment of the CDs into the polymeric network of polyvinyl alcohol and polyvinyl pyrrolidone resulted in the enhancement of emission in CDs which facilitated the solid-state generation of the white light of a LED chip using a gallium nitride UV LED at 30 V. They further demonstrated the use of a CD/PVDF (PVDF = polyvinylidene fluoride polymer) nanocomposite as a heterogeneous catalyst for the reduction of resazurin and 2.4-dinitrophenol to resorufin and aminophenol, in the presence of N_2H_4 and $NaBH_4$, respectively (Fig. 19) [115].

Momper [116] and Li [117] stabilized CDs using polystyrene (PS) nanoparticles and a hollow molecularly imprinted polymer (HMIP), respectively. The CDs on a polymeric network were investigated by observing the fluorescence emission of the CDs when varying the pH of the solution. The commonality in their studies was, (i) under acidic conditions the fluorescence emission of CDs was low, (ii) under basic conditions the fluorescence emission of CDs was enhanced, and (iii) at neutral pH the fluorescence emission was quenched. They concluded that the surface states in the CDs were the main constituents responsible for the fluorescent emissions. At the lower and higher pH, the polymeric network matrix was protonated and deprotonated to exhibit different interactions between the polymer and the CDs. As such, the polymeric network interactions with CDs played a role in stabilizing the surface traps and suppressing the non-radiative recombination of the excited states [116,117].

As shown in Fig. 20, Momper used the CD-PS nanocomposite as a biomarker for labeling Hella cells which had good biocompatibility. The CD-PS exhibited enhanced emission labeling of Hella cells as seen by the fluorescence contrast images taken by a confocal laser scanning microscopy (CLSM) at excitation wavelengths of 415 and 524 nm [116]. Li used the HMIP/CD nanocomposite for the detection of tetracycline (TC) in honey which exhibited good sensitivity and strong interaction toward the TC. These nanocomposites showed poor selectivity when compared to their TC analogs, but no interference when metal ions, amino acids, and vitamins were present in the honey used [117].

Ahmed and Yu demonstrated the use of CD/polymeric-supported nanocomposites as probes for the detection of picric acid and citrate, respectively [118,119]. Ahmed demonstrated a hydrothermal treatment of gelatin to produce CDs which were supported on a polyaniline (PANI) polymeric network (CD/PANI). In this study, the effect of annealing temperature and polymerization time on the CD/PANI nanocomposites was investigated and it was observed that increasing annealing temperature and aniline polymerization resulted in quenching of the fluorescence emission of the CDs. These observations were due to fluorescence resonance energy transfer (FRET) in which the PANI pi-systems acted as an acceptor resulting in non-radiative decay of these

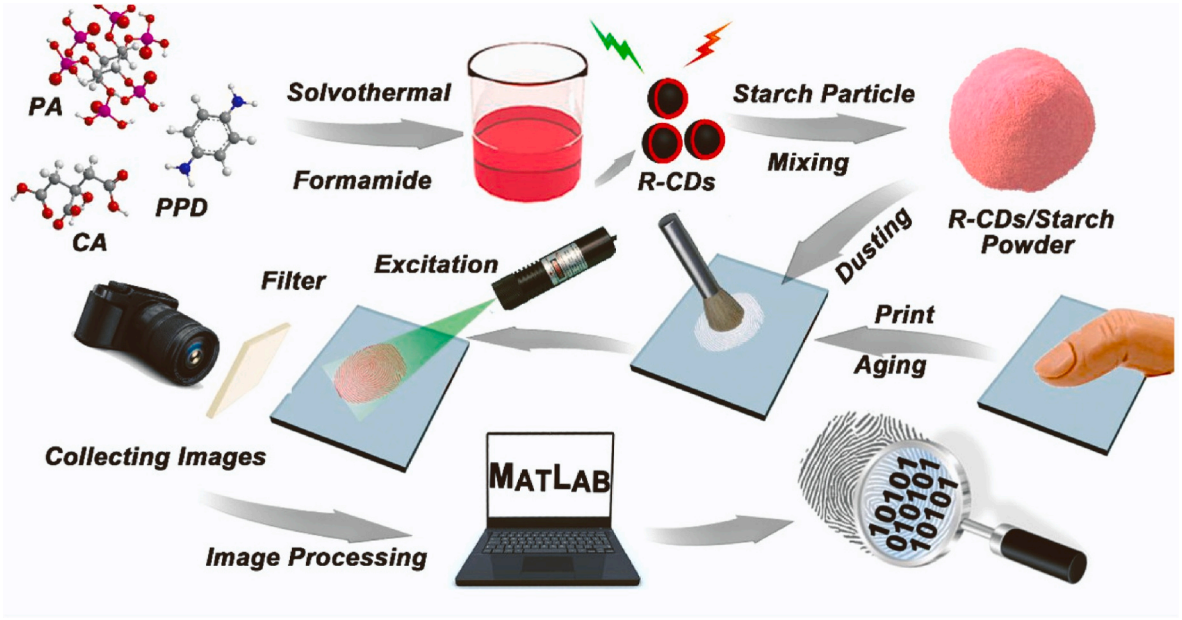

Fig. 14. Preparation Process of R-CDs/Starch Powder and Its Application in LFP Detection, (Adapted with permission from American Chemical Journal, 2020) [105].

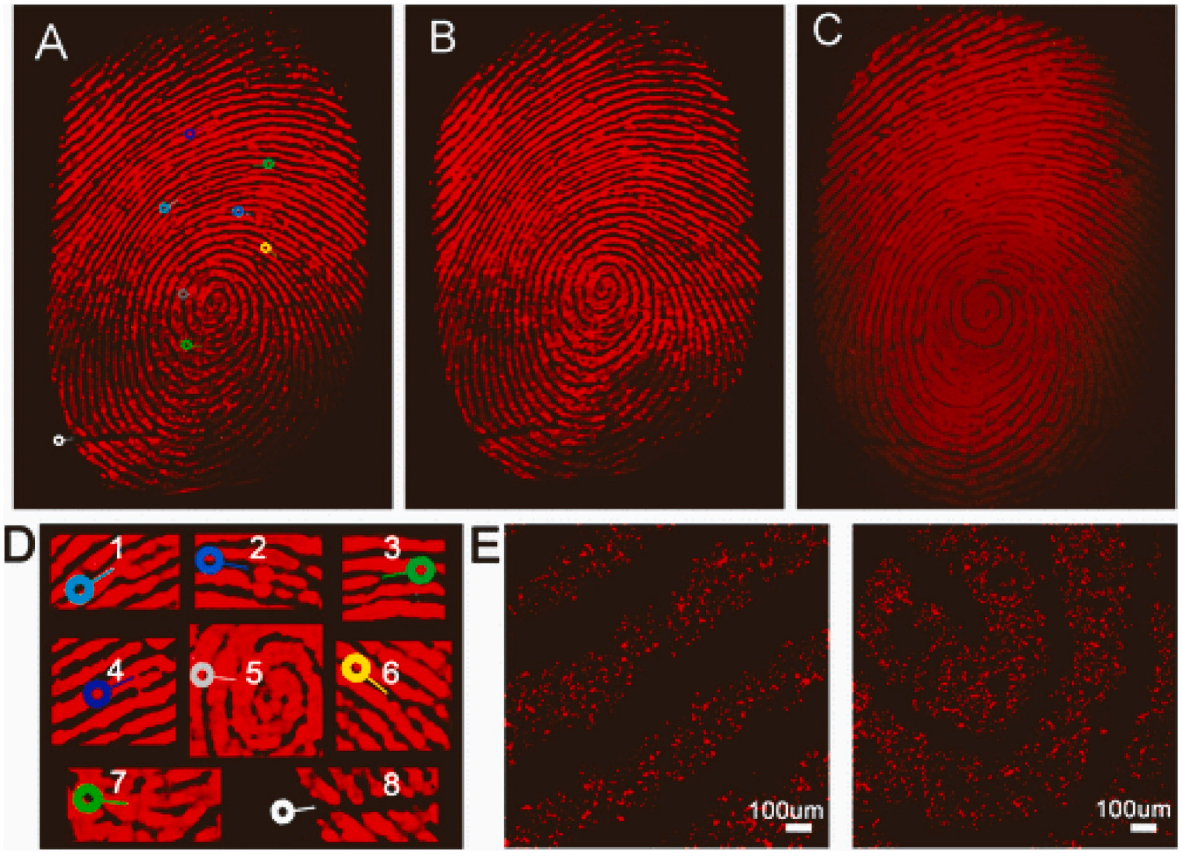

Fig. 15. Photographs of the R-CDs/starch phosphor-stained LFPs on (A) glass, (B) paper, and (C) plastic substrates under green light irradiation, respectively. (D) Magnified images showing eight kinds of details as marked in A, that is, (1) bifurcation, (2) island, (3) termination, (4) eye, (5) core, (6) ridge divergence, (7) crossover, and (8) scar. Confocal fluorescence images of (E) R-CDs/starch-stained fingerprints on a glass sheet and (F) the same sample after several weeks' storage, (Adapted with permission from American Chemical Journal, 2020) [105].

excited states. In addition, the lifetime decay of the excited states was decreased due to a decrease in electron delocalization of the CDs by the PANI polymeric structure. These CD/PANI nanocomposites showed good sensitivity and selectivity for picric acid detection and a mechanism of action for fluorescence quenching was proposed to be due to the transfer of excited electrons from the CDs to the HOMO of the picric acid which resulted in nonradiative decay [118].

The use of CD-doped terbium coordinated on a polymeric network

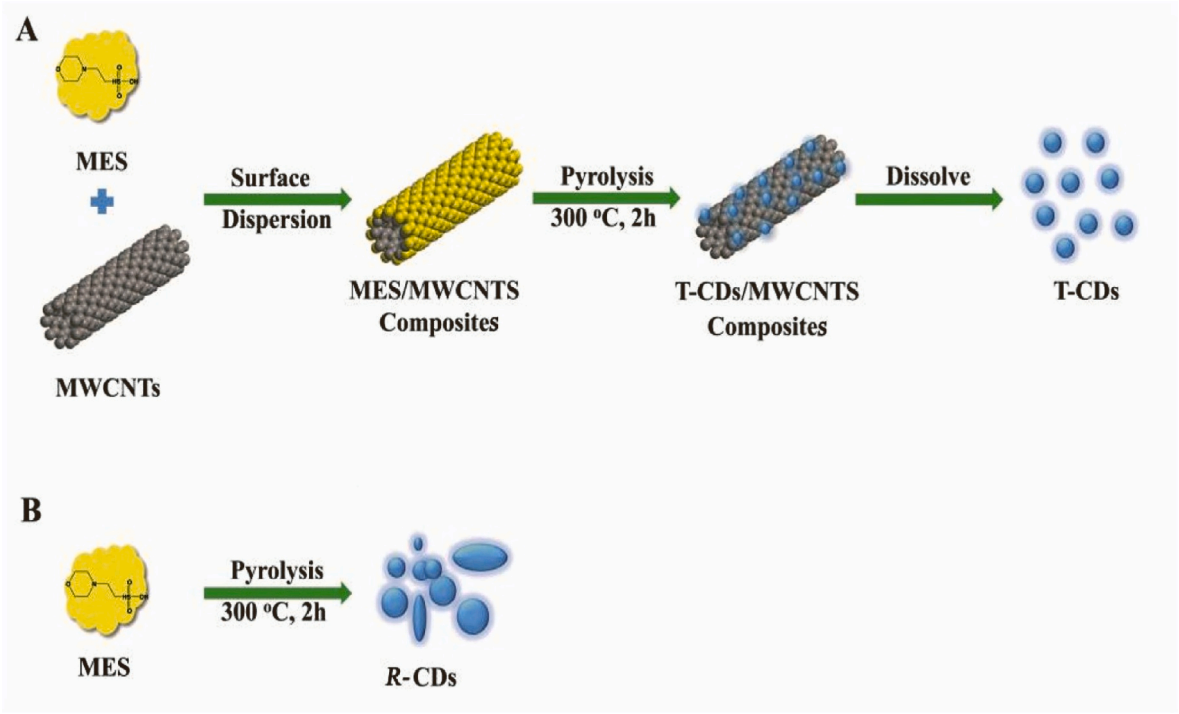

Fig. 16. Schematic representation for the synthesis of (A) CDs using MWCNTs as support and (B) CDs synthesized without MWCNTs support, (Adapted with permission from Elsevier, copyright 2019 [109].

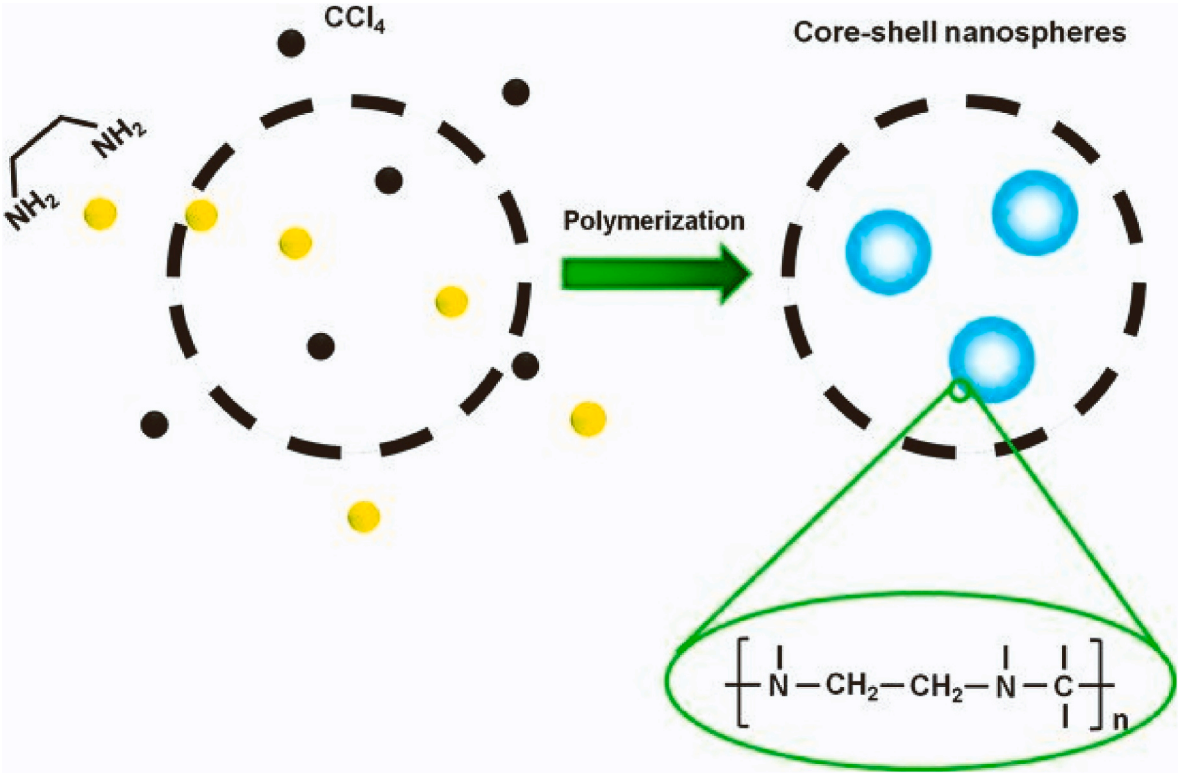

Fig. 17. A core-shell procedure for preparation of CD@HCSs nanocomposite, (Adopted with permission from Wiley-VCH Verlag GmbH & Co, copyright 2012) [110].

made of guanosine-5-monophosphate (GMP) ligands (CD-GMP/Tb nanocomposite) for the detection of citrate was observed to enhance the fluorescence emission in CDs as the CD concentration was increased. This was associated with the stabilization of excited states on the CDs, which resulted in a prolonged lifetime of the nanocomposite from 76.95 μs to 630.80 μs upon the addition of citrate. The nanocomposite showed a rapid detection of the citrate in the range of 0–200 μM, having a limit of detection of 0.47 μM and a correlation coefficient of 0.9986. These nanocomposites could also be used for the imaging and detection of citrate in living cells (HepG-2 cells) in which the incubation of living

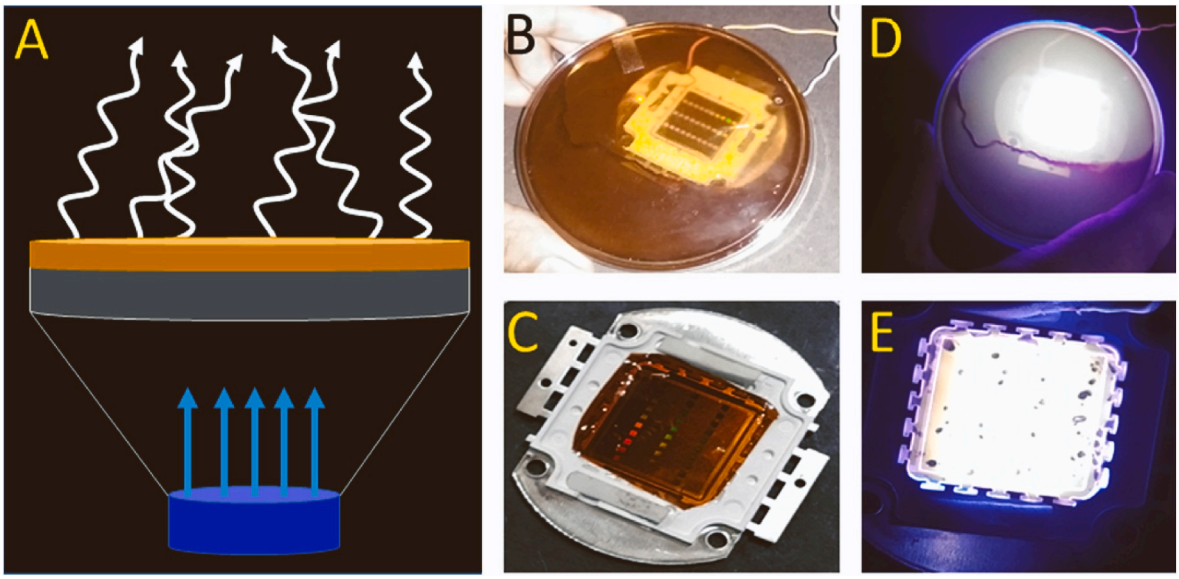

Fig. 18. Schematic representation of the generation of white light using an LED chip, (B–C) and (D–E) ambient light, and GaN UV LED at 30 V observation of CD/PVA/PVP films on the LED chip, (Adapted with permission from Elsevier, copyright 2022) [115].

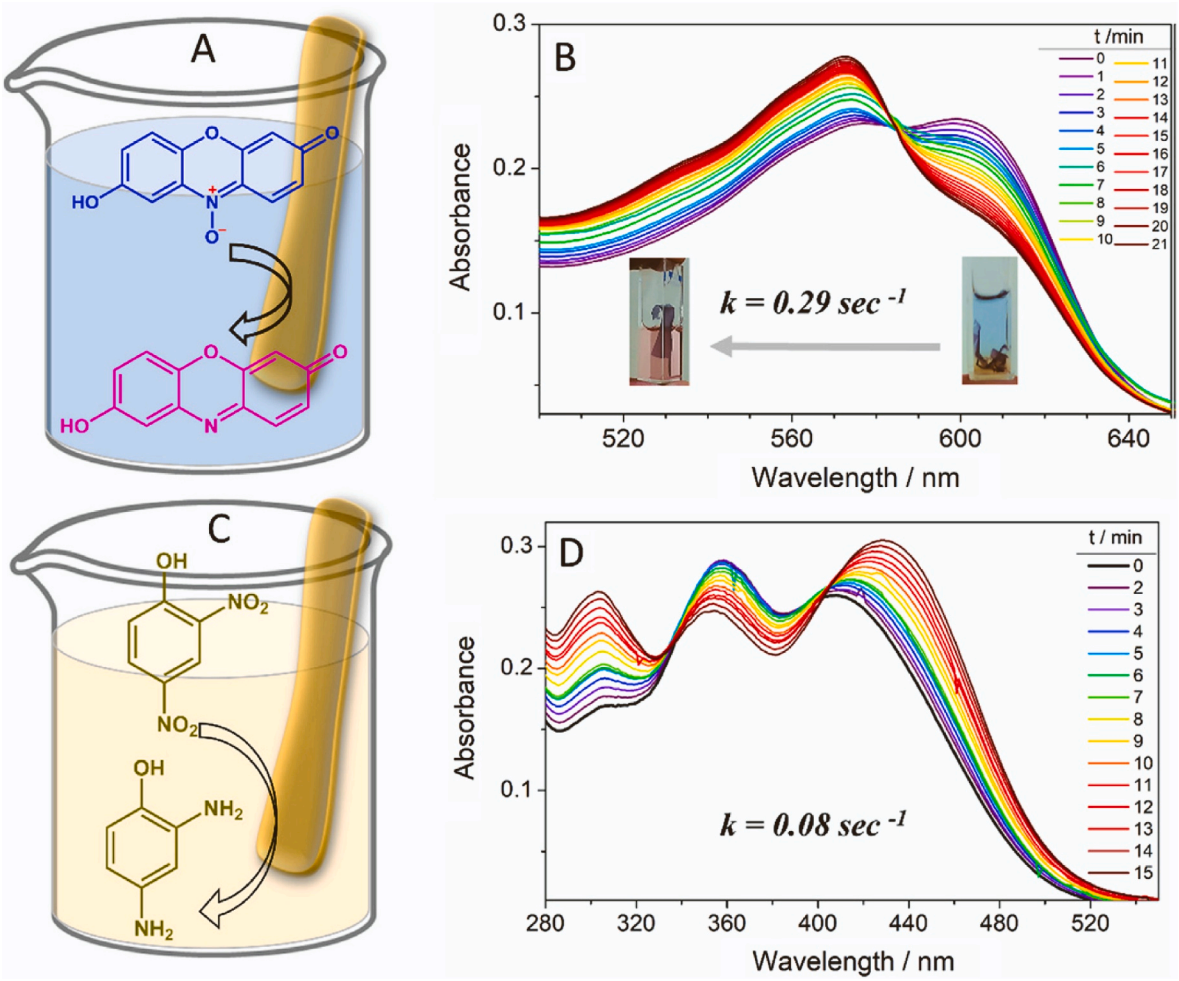

Fig. 19. (A) Schematic representation for catalytic reduction of resorufin, (B) catalytic conversion of resorufin recorded using UV–vis, (C) Schematic representation for catalytic reduction of 2.4-dinitrophenol (D) UV–Vis spectra for catalytic conversion of 2.4-dinitrophenol, (catalytic reduction were carried using CD/PVDF nanocatalyst), (Adapted with permission from Elsevier, copyright 2022) [115].

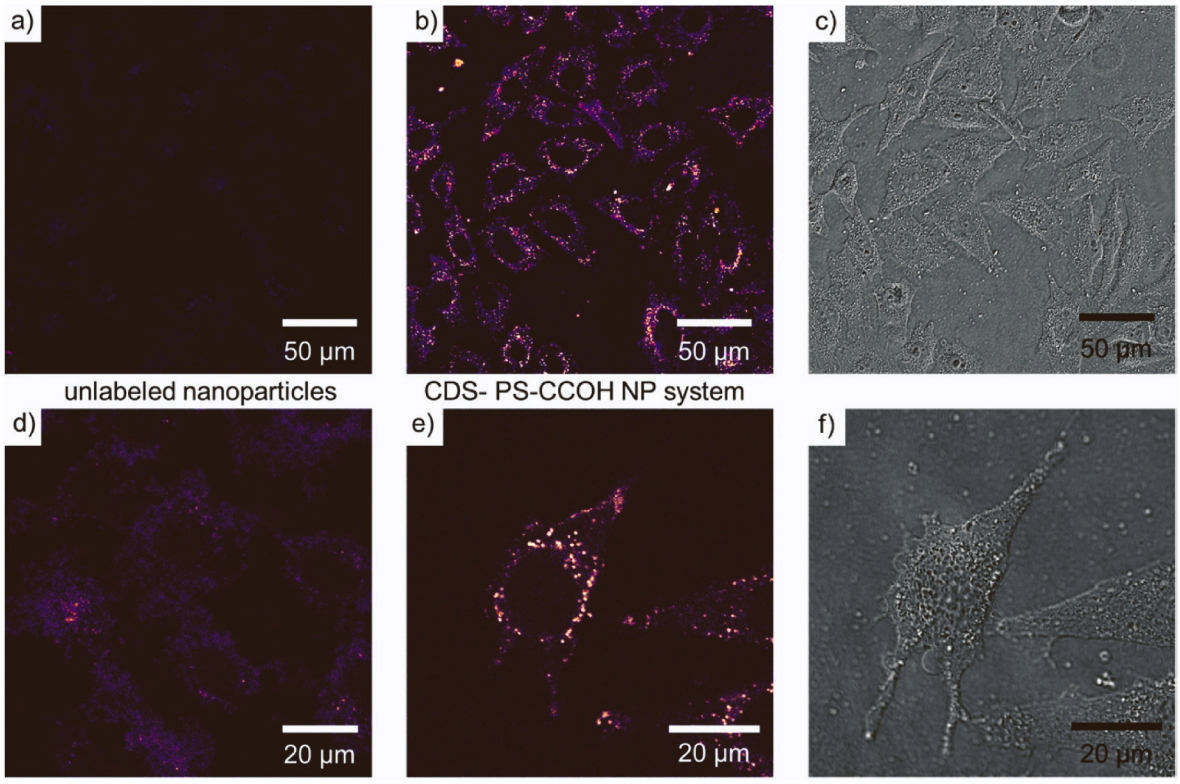

Fig. 20. Tracing of CDS-fluorescently labeled nanoparticles during their cellular uptake. Microscope images of Hella cells incubated with carboxyl functionalized polystyrene (PS–COOH) nanoparticles. (a, d) PS-COOH nanoparticles; (b, c, e, f) PS-COOH nanoparticles labeled with carbon dots (by in situ formation, CDS-PS COOH NP); left side: (a, b, d, e) fluorescence contrast images taken by CLSM (λ = 415–524 nm); right side: (c, f) DIC images, (Adopted with permission from Elsevier Inc, copyright 2018) [116].

cells with citrate resulted in green light quenching with the enhancement of blue light fluorescence emission.

Mahmoud and co-workers demonstrated the formation of ester covalent bonds between hydroxyl groups on CDs and polymer network carboxyl groups. The polymer network (PAFP) was obtained by using anthranilic acid, formaldehyde, and phthalic acid. The formation of a covalent bond in the CD/PAFP nanocomposite suppressed water solubility in CDs. It was used for the adsorption of uranium (U) ions under microwave irradiation (30 s) and allowed for easy recovery and reuse (five times) of the composite, This nanocomposite/nanobiosorbent showed good selectivity toward U in the presence of species such as KCl, NH_4Cl, NaCl, $CaCl_2$, and $MgSO_4$ [120]. A study by Zhai and co-workers used a three-dimensional polyacrylamide (PAM) polymer to confine CDs. The CD/PAM nanocomposite was used as a room temperature phosphorescence (RTP) material. These nanocomposites showed ultralong lifetime phosphorescence and were not quenched by solvents (e.g. ethanol, DMSO, DMF, THF, etc.) but rather by varying crosslinker and temperature. The lifetime of the RTP changed from 315.44 ms to 577.2 ms with temperature (in the range of 30 °C–120 °C), and varying crosslinkers also increased the lifetime of the RTP. This was due to the confinement of the CDs in the polymer matrix. In addition, the nanocomposite was photostable under an oxygen environment and in various pH ranges. However, the humidity was found to decrease the RTP lifetime due to the weakening of hydrogen bonds between the CDs and the polymer. As shown in Fig. 21, the CD/PAM nanocomposites were used for the preparation of a flexible RTP fiber. The preparation of the nanocomposite-coated fibers was achieved by, (i) coating the cotton fiber with the nanocomposite and (ii) in situ crosslinking and drying the composite. The obtained RTP fiber was used to design an RTP material with good stability with potential for practical application and production scaling [121].

Since 2013, CDs have gained momentum for application in energy storage materials. In hybrid supercapacitors application, Wei et al. demonstrated the use of CDs supported on polyacrylamide (PAM) hydrogel composite. As shown in Fig. 22, the N,P,O co-doped CDs were combined with PAM hydrogel and annealed under an N_2 environment to obtain CDs/HPC nanocomposites, (HPC = Hierarchical porous carbon). The presence of CDs facilitated the introduction of abundant functional groups such as C–N, pyridic N, phosphate groups, and carboxyl groups, and led to defined pore distribution, higher surface area, and electron-rich regions. The presence of the functional groups facilitated the generation of a change in charge in the surrounding atoms. When used as a negative electrode to a fabricated hybrid supercapacitor, the nanocomposite could reach specific a capacitance of 468, 510, and 438 F/g in alkaline, acidic and neutral electrolytes. In addition, the composites reached an energy density of up to 90 Wh/Kg with 100% capacity retention after 10 000 cycles. These observations were correlated to the presence of the functional groups from CDs which facilitated the formation of electron-rich regions on the electrode surface to absorb more cations [122]. This overcomes drawbacks, such as self-discharge, that can be experienced in carbon-negative electrodes [123]. Although the nanocomposite had the promising potential for use as a negative electrode further investigations are essential for it to find practical application.

Wei et al. have summarized the use of CDs as a building unit for the construction and preparation of energy storage materials. Since 2013, the CDs have been incorporated into various support matrices for use in energy storage devices such as Li-ion batteries, supercapacitors, Na-ion batteries, flow batteries, K-ion batteries, etc. The literature provides vivid guidance and a recent update on the advantages of integrating CDs in energy storage devices. This includes but is not limited to the role that CDs play in CDs/support nanocomposites such as acting as an influence on structural design, providing active sites, increasing surface area, and enhancing wettability, among others. The summarized literature

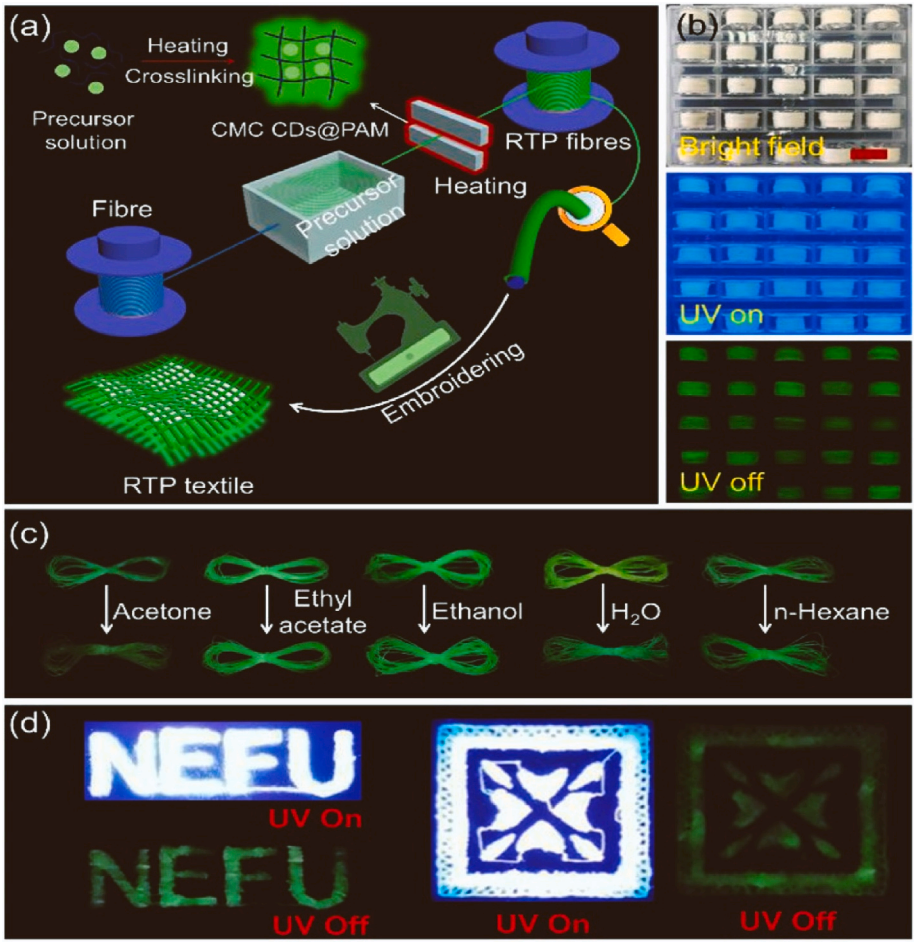

Fig. 21. Application of CMC CD@PAM. (a) Schematic illustration of the preparation of RTP fibers via homemade apparatus. (b) Digital images of RTP fibers under bright field, UV irradiation, and after turning off the UV sources, scale bar = 1 cm. (c) RTP emission of fiber before and after treatment of the corresponding solvent for 24 h (The photo was taken after drying the treated fibers at 60 °C for 2 h). (d) Digital images of embroidery upon and after UV excitation, (Adapted with permission from Elsevier, copyright 2022) [121].

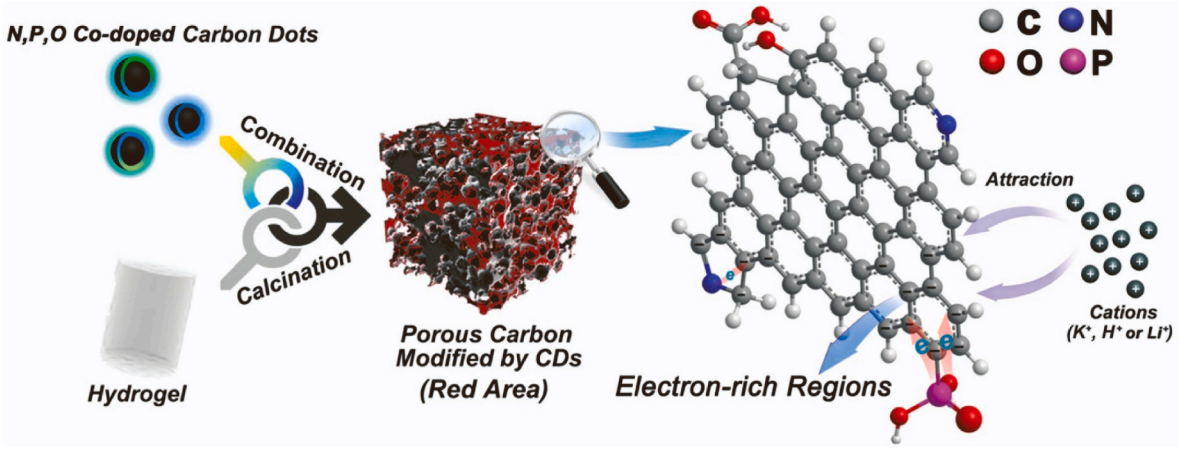

Fig. 22. The porous carbon was derived from carbon dots and PAM hydrogels. This material has plenty of functional groups and electron-rich defects for cations adsorption/reaction, (Adapted with permission from WILEY-VCH Verlag GmbH & Co. KGaA, Weinheim, 2018) [122].

suggests that the presence of CDs can enhance the electrolyte ion transport, specific capacitance, electrical conductivity, and generation of a change in charge in the surrounding atoms due to functional groups or building electron-rich regions which in turn improve the electrochemical performance of the energy storage devices [124].

CDs/C_3N_4 nanocomposites: Carbon nitride has been explored as a metal-free photocatalyst that can be used for the production of hydrogen, and in photodegradation reactions. It can be synthesized by pyrolysis of urea and/or melamine and can be used in heterojunction devices. Direct deposition of CDs or carbon quantum dots (CQDs) onto a bulk C_3N_4 facilitated the light absorption of the photocatalyst, reduced the recombination of electron-hole pairs, and induced a higher transfer of photoinduced charge carriers suitable for H_2 production [125]. In an attempt to explore the use of graphitic nitride as a metal-free catalyst, a nanocomposite consisting of proton-functionalized graphitic nitrides (HpCN) and CQDs was prepared via an electrostatic self-assembly approach. When compared to HpCN, the CQD/HpCN nanocomposite exhibited a strong absorption peak that extended toward the visible

region suggesting the absorption of more energy and an enhanced photoactivity of the nanocomposite. The CQD/HpCN nanocomposite exhibited an enhanced photocurrent density of 1.89 μAcm^{-2} as compared to 1.14 μAcm^{-2} for HpCN, due to a synergistic effect between the CDs and the HpCN. The nanocomposite showed higher photodegradation of methylene blue under visible light with good stability after 5 cycles. The higher photocatalytic efficiency was attributed to the enhanced electronic conductivity, and higher electron transfer facilitated by the supported CQDs [126].

An in-depth evaluation of a CD/C_3N_4 nanocomposite was used to probe the detection of metal ions in wastewater. The fluorescence intensity of the supported CDs was enhanced as the metal ion concentration was increased. As shown in Fig. 23, the CD/C_3N_4 nanocomposite's fluorescence intensity was quenched by the C_3N_4 support matrix. Interestingly, when the metal ions (Cr (VI), Cu (II), and Pb (II)) were added to the nanocomposites the fluorescence intensity of the CDs was enhanced. The mechanism of action for this atypical observation was related to the surface charge of the CDs (positive) and the C_3N_4. It is known that graphitic C_3N_4 is a good metal ion adsorbent. The electrostatic repulsion between the metal ions, the C_3N_4 complex, and the CDs resulted in the CDs being released from the C_3N_4. Thereafter, the released CDs exhibited a fluorescence intensity that was directly proportional to the metal ion concentration. As such the C_3N_4 nanosheets acted as a good fluorescence quencher and recognized a range of metal ions, with a good limit of detection of 0.54, 0.18, and 0.2 nM for Cr (VI), Cu (II), and Pb (II), respectively [127].

5.5. TiO_2

The advantages of TiO_2 as a photocatalyst have been demonstrated by its properties such as its indirect small bandgap (3.2 eV), chemical stability, high reactivity, porosity, natural abundance, low cost, and low toxicity [128,129]. However, TiO_2 has limitations as a photocatalyst that range from (i) an inability to utilize enough of the solar spectrum energy (i.e., it can only utilize 5%), (ii) fast recombination of electron-hole pairs, and (iii) agglomeration of the TiO_2 nanoparticles. The use of CDs as a sorbent on the surface of TiO_2 has been shown to improve the photocatalytic activity of the TiO_2 photocatalyst. This is due to the CDs acting as an electron reservoir which improved the separation of the generated electron/hole, to make it act as a good photosensitizer for the catalyst. For example, CD/TiO_2 nanocomposites were observed to utilize the light characteristics from CDs to activate the TiO_2 catalyst which enhanced the photocatalytic conversion of an analyte of interest into the desired product [130]. It was also observed that CDs supported on the surface of N-doped-TiO_2 nanorods improved the electrochemical performance when the nanocomposite was used as an anode material in sodium-ion batteries [131]. The proposed mechanism in which the CDs improved the photocatalytic hydrogen evolution when supported onto TiO_2–P25, is shown in Fig. 24. The CDs on the CD/P25 nanocomposite were observed to have dual actions. Thus, (i) under UV light irradiation (450 nm) the CDs played the role of an electron reservoir to trap excited electrons from the conduction band of the catalyst, and this facilitated the separation of the generated electron-hole pairs, and (ii) when visible

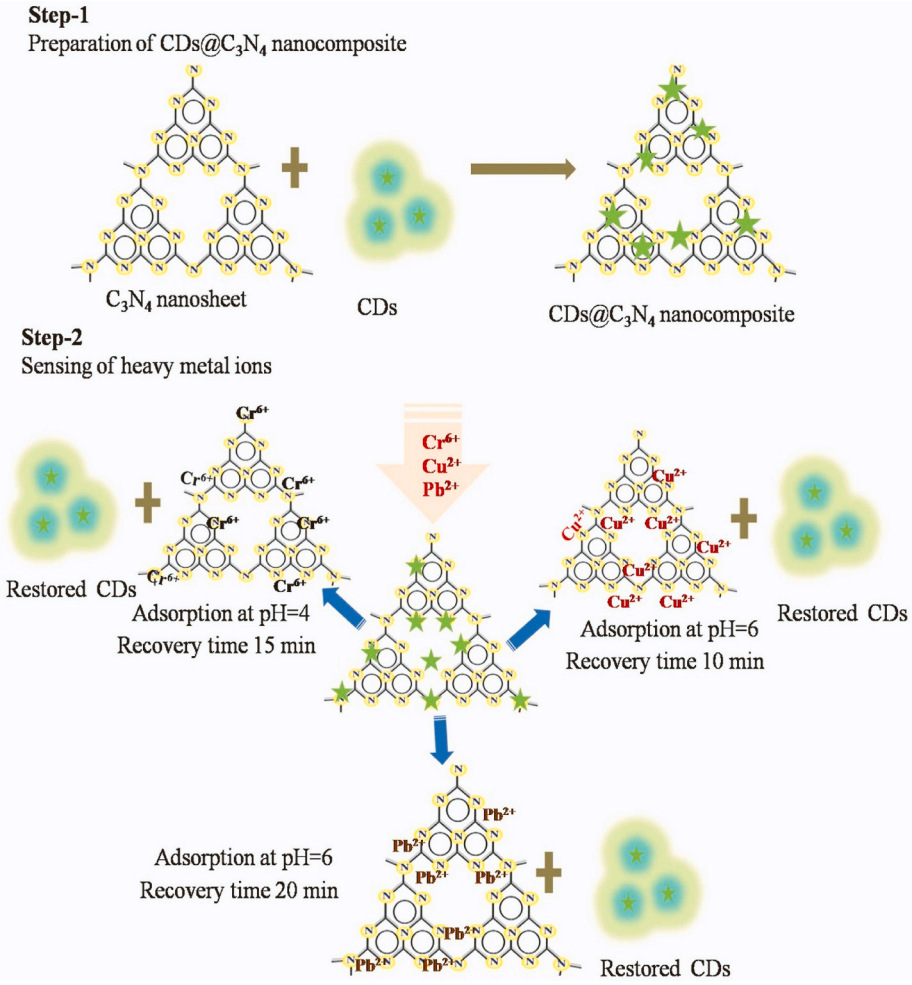

Fig. 23. Schematic illustration to represent the design and working principle of CD@g-C_3N_4 nanocomposite, (Adopted with permission from Elsevier B.V, copyright 2019) [127].

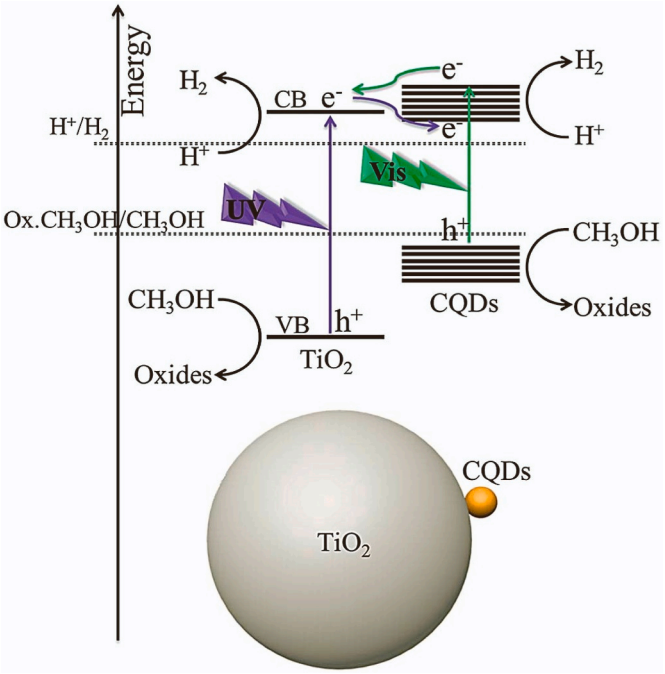

Fig. 24. Proposed mechanism for a CD/P25 nanocomposite under UV–vis and visible light irradiation, (H_2 production mechanism), (Adopted with permission from Royal Society of Chemistry, copyright 2012) [132].

light was used, the CDs acted as a photosensitizer resulting in the catalyst being responsive to visible light that allowed injection of electrons from the CDs to the conduction band of the catalyst [132]. These observations, provide important information for the utilization and design of CD-based nanocomposites for use in photocatalytic hydrogen production, dye degradation, electrochemistry, and photonics.

The electron transferability exhibited by the CDs is known to suppress the recombination of photogenerated electron-hole pairs. Thus, the CDs were decorated onto TiO_2 nanoparticles and TiO_2 nanotube arrays (TNTA) by Vu Nu, and Wei, together with their co-workers, respectively. Vu Nu and co-workers used microalgae as a precursor for the synthesis of CDs. These CDs were decorated on the surface of the TiO_2 using a microwave-assisted method. Wei and co-workers demonstrated a one-step solvothermal method for the synthesis of their AgNp/CD/TNTA nanocomposites. In both studies, the authors used their nanocomposites (CD/TiO_2 and Ag/CD/TNTA) for the photodegradation of methylene blue from water. They both concluded that the presence of the CDs on the TiO_2 nanoparticles and TNTA enhanced the light absorption of the nanocomposites and suppressed the recombination of photogenerated electron-hole pairs. In addition, the incorporation of microalgae-based CDs resulted in a reduction of the bandgap of TiO_2 and the CDs also acted as an electron reservoir for trapping photoinduced electrons. The CDs on the Ag/CD/TNTA nanocomposites favored the transfer of electrons between AgNp, CDs, and TNTA and resulted in the enhanced photodegradation of methylene blue [133,134]. The electrical properties of the CDs were also explored on CD/support nanocomposites. In this case, the presence of CDs derived from citrate in a titania P25-CDs nanocomposite exhibited an enhanced photocatalytic hydrogen evolution performance, reaching up to 7-fold higher than pristine P25. The enhancement of hydrogen evolution was ascribed to the higher electrical conductivity of CDs that resulted in the fast separation of electrons and holes.[135]

6. Summary

The fluorescence quenching that occurs when the CDs physical state is changed from solution to solid/powder can be a result of a direct π-π interaction of the core structure, excessive resonance energy transfer, or electron delocalization that can be caused by the reduced distance between adjacent CDs. Hence, an understanding of the use of the support matrices is pivotal to circumvent the drawbacks that are experienced when solid/powder CDs are used in fluorescence studies. The properties of the composites will be dependent on both the CD type and the support material. Depending on the synthesis method, the interaction between CDs and the support matrices can be via covalent bonding, a physical surface interface interaction, hydrogen bonding, or π-π interactions. Thus, the review has indicated i) the types of CDs that can be supported, ii) the types of supports used to date, iii) the CD-support interaction, and iv) the properties that emerge from the CD-support interaction. In particular, the emphasis on the role of the support matrix in the CD-support nanocomposites has been indicated, with emphasis on the fluorescence emissions of the resultant supported CDs. Various support matrices such as silica, zeolites, polymers, structured carbons, titania, and xerogels, alloys have been used. Many other supports can be envisaged that could be used to make the CD-composites. The improved properties of the supported/confined CDs such as induced light absorption properties, electron transfer rates, photoluminescence intensity, the introduction of abundant functional groups, biocompatibility, lower toxicity, and bandgap tuning were highlighted. The fields in which the CD-support nanocomposites have been studied were outlined and reviewed and included optoelectronic devices, water treatment, photoreactions, electrochemistry, nanomedicine, sensors, bioimaging, energy storage, and catalysis. Although the CD-support nanocomposites have been demonstrated to be good candidates for applications in various fields, there are still issues that need to be resolved with the CD-support materials. These include detailed literature on the effect that the type of CDs, their particle sizes and the nature of interactions (covalent or noncovalent interactions) that influences the optoelectronic properties of nanocomposites. The fundamental knowledge that correlates the synthesis method, and surface states to the upconversion photoluminescence of the nanocomposites is lacking.

Credit author statement

Orlette Mkhari: Conceptualization, writing-Original draft. Themba D Ntuli, Neil J Coville, Manoko S Maubane-Nkadimeng and Edward N Nxumalo: Conceptualization, reviewing and editing, and resources. All the authors have contributed by reading, editing and confirmed to publication of this review.

Declaration of competing interest

The authors declare that they have no known competing financial interests or personal relationships that could have appeared to influence the work reported in this paper.

Data availability

No data was used for the research described in the article.

Acknowledgments

We wish to acknowledge financial support from the National Research Foundation (NRF) of South Africa (Grant numbers: 118137 and 113906), the DSI-NRF Centre of Excellence in Strong Materials and the University of The Witwatersrand.

References

[1] X. Jia, J. Li, E. Wang, One-pot green synthesis of optically pH-sensitive carbon dots with upconversion luminescence, Nanoscale 4 (18) (2012) 5572–5575.
[2] R. Jelinek, Carbon Quantum Dots, Carbon quantum dots, Springer International Publishing, Cham, 2017, pp. 29–46.

[3] M. Kurian, A. Paul, Recent trends in the use of green sources for carbon dot synthesis–A short review, Carbon Trends 3 (2021), 100032.
[4] A.L. Himaja, P.S. Karthik, S.P. Singh, Carbon dots: the newest member of the carbon nanomaterials family, Chem. Rec. 15 (3) (2015) 595–615.
[5] P. Zhao, L. Zhu, Dispersibility of carbon dots in aqueous and/or organic solvents, Chem. Commun. 54 (43) (2018) 5401–5406.
[6] F. Yuan, S. Li, Z. Fan, X. Meng, L. Fan, S. Yang, Shining carbon dots: synthesis and biomedical and optoelectronic applications, Nano Today 11 (5) (2016) 565–586.
[7] L.I. Cao, M.J. Meziani, S. Sahu, Y.P. Sun, Photoluminescence properties of graphene versus other carbon nanomaterials, Acc. Chem. Res. 46 (1) (2013) 171–180.
[8] M. Tuerhong, X.U. Yang, Y.I.N. Xue-Bo, Review on carbon dots and their applications, Chin. J. Anal. Chem. 45 (1) (2017) 139–150.
[9] B. Zhang, F. Wang, H. Zhou, D. Gao, Z. Yuan, C. Wu, X. Zhang, Polymer dots compartmentalized in liposomes as a photocatalyst for in situ hydrogen therapy, Angew. Chem. Int. Ed. 58 (9) (2019) 2744–2748.
[10] L.L. Mokoloko, R.P. Forbes, N.J. Coville, The transformation of 0-D carbon dots into 1-, 2-and 3-D carbon allotropes: a minireview, Nanomaterials 12 (15) (2022) 2515.
[11] C. Xia, S. Zhu, T. Feng, M. Yang, B. Yang, Evolution and synthesis of carbon dots: from carbon dots to carbonized polymer dots, Adv. Sci. 6 (23) (2019), 1901316.
[12] H. Ding, X.X. Zhou, J.S. Wei, X.B. Li, B.T. Qin, X.B. Chen, H.M. Xiong, Carbon dots with red/near-infrared emissions and their intrinsic merits for biomedical applications, Carbon 167 (2020) 322–344.
[13] Q. Liang, W. Ma, Y. Shi, Z. Li, X. Yang, Easy synthesis of highly fluorescent carbon quantum dots from gelatin and their luminescent properties and applications, Carbon 60 (2013) 421–428.
[14] K. Hola, A.B. Bourlinos, O. Kozak, K. Berka, K.M. Siskova, M. Havrdova, J. Tucek, K. Safarova, M. Otyepka, E.P. Giannelis, R. Zboril, Photoluminescence effects of graphitic core size and surface functional groups in carbon dots: COO− induced red-shift emission, Carbon 70 (2014) 279–286.
[15] F.R. Baptista, S.A. Belhout, S. Giordani, S.J. Quinn, Recent developments in carbon nanomaterial sensors, Chem. Soc. Rev. 44 (13) (2015) 4433–4453.
[16] H. Yu, Y. Zhao, C. Zhou, L. Shang, Y. Peng, Y. Cao, L.Z. Wu, C.H. Tung, T. Zhang, Carbon quantum dots/TiO 2 composites for efficient photocatalytic hydrogen evolution, J. Mater. Chem. 2 (10) (2014) 3344–3351.
[17] X.T. Zheng, A. Ananthanarayanan, K.Q. Luo, P. Chen, Glowing graphene quantum dots and carbon dots: properties, syntheses, and biological applications, Small 11 (14) (2015) 1620–1636.
[18] M. Moniruzzaman, J. Kim, N-doped carbon dots with tunable emission for multifaceted application: solvatochromism, moisture sensing, pH sensing, and solid state multicolor lighting, Sensor. Actuator. B Chem. 295 (2019) 12–21.
[19] D. Zhou, D. Li, P. Jing, Y. Zhai, D. Shen, S. Qu, A.L. Rogach, Conquering aggregation-induced solid-state luminescence quenching of carbon dots through a carbon dots-triggered silica gelation process, Chem. Mater. 29 (4) (2017) 1779–1787.
[20] Y. Chen, M. Zheng, Y. Xiao, H. Dong, H. Zhang, J. Zhuang, H. Hu, B. Lei, Y. Liu, A self-quenching-resistant carbon-dot powder with tunable solid-state fluorescence and construction of dual-fluorescence morphologies for white light-emission, Adv. Mater. 28 (2) (2016) 312–318.
[21] B.T. Zhang, Q. Wang, Y. Zhang, Y. Teng, M. Fan, Degradation of ibuprofen in the carbon dots/Fe3O4@ carbon sphere pomegranate-like composites activated persulfate system, Separ. Purif. Technol. 242 (2020), 116820.
[22] G.A. Hutton, B.C. Martindale, E. Reisner, Carbon dots as photosensitisers for solar-driven catalysis, Chemical Society Reviews 46 (20) (2017) 6111–6123.
[23] G. Zhang, Q. Ji, Z. Wu, G. Wang, H. Liu, J. Qu, J. Li, Facile "spot-heating" synthesis of carbon dots/carbon nitride for solar hydrogen evolution synchronously with contaminant decomposition, Advanced Functional Materials 28 (14) (2018), 1706462.
[24] Y. Deng, Y. Ji, F. Chen, F. Ren, S. Tan, Superior performance of flexible solid-state supercapacitors enabled by ultrafine graphene quantum dot-decorated porous carbon spheres, New Journal of Chemistry 44 (32) (2020) 13591–13597.
[25] S. Gogoi, N. Karak, Solar-driven hydrogen peroxide production using polymer-supported carbon dots as heterogeneous catalyst, Nano-micro letters 9 (4) (2017) 1–11.
[26] L. Zhou, Z. Li, Z. Liu, J. Ren, X. Qu, Luminescent carbon dot-gated nanovehicles for pH-triggered intracellular controlled release and imaging, Langmuir 29 (21) (2013) 6396–6403.
[27] M. Esmaeilzadeh, S. Sadjadi, Z. Salehi, Pd immobilized on hybrid of magnetic graphene quantum dots and cyclodextrin decorated chitosan: an efficient hydrogenation catalyst, International journal of biological macromolecules 150 (2020) 441–448.
[28] X. Zhao, A. Wang, S. Gao, D. Yan, W. Guo, Y. Xu, Y. Meng, C. Wang, G. Shan, Enhancing photoluminescence of carbon quantum dots doped PVA films with randomly dispersed silica microspheres, Scientific reports 10 (1) (2020) 1–10.
[29] Zhu, S., Song, Y., Zhao, X., Shao, J., Zhang, J., and Yang B. The photoluminescence mechanism in carbon dots (graphene quantum dots, carbon nanodots, and polymer dots): current state and future perspective. Nano Research vol. 8 pp.355–381.
[30] Y. Wang, A. Hu, Carbon quantum dots: synthesis, properties and applications, Journal of Materials Chemistry C 2 (34) (2014) 6921–6939.
[31] S. Tajik, Z. Dourandish, K. Zhang, H. Beitollahi, Q. Van Le, H.W. Jang, M. Shokouhimehr, Carbon and graphene quantum dots: a review on syntheses, characterization, biological and sensing applications for neurotransmitter determination, RSC advances 10 (26) (2020) 15406–15429.
[32] P. Roy, P.C. Chen, A.P. Periasamy, Y.N. Chen, H.T. Chang, Photoluminescent carbon nanodots: synthesis, physicochemical properties and analytical applications, Materials Today 18 (8) (2015) 447–458.
[33] Y. Dong, L. Wan, J. Cai, Q. Fang, Y. Chi, G. Chen, Natural carbon-based dots from humic substances, Scientific reports 5 (1) (2015) 1–8.
[34] S. Muramulla, H.D. Arman, C.G. Zhao, E.R. Tiekink, 1-[3, 5-Bis (trifluoromethyl) phenyl]-3-[(5-ethenyl-1-azabicyclo [2.2. 2] octan-2-yl)(6-methoxyquinolin-4-yl) methyl] thiourea–l-proline–methanol (1/1/1), Acta Crystallographica Section E: Structure Reports Online 65 (12) (2009) o3070, o3070.
[35] F. Yuan, S. Li, Z. Fan, X. Meng, L. Fan, S. Yang, Shining carbon dots: synthesis and biomedical and optoelectronic applications, Nano Today 11 (5) (2016) 565–586.
[36] F. Yan, Y. Jiang, X. Sun, J. Wei, L. Chen, Y. Zhang, Multicolor carbon dots with concentration-tunable fluorescence and solvent-affected aggregation states for white light-emitting diodes, Nano Research 13 (1) (2020) 52–60.
[37] X.F.L. Jia, E.K. Wang, One-pot green synthesis of optically pH-sensitive carbon dots with upconversion luminescence, Nanoscale 4 (2012) 5572–5575, 2012.
[38] D. Li, E.V. Ushakova, A.L. Rogach, S. Qu, Optical properties of carbon dots in the deep-red to near-infrared region are attractive for biomedical applications, Small 17 (43) (2021), 2102325.
[39] A. Zhao, Z. Chen, C. Zhao, N. Gao, J. Ren, X. Qu, Recent advances in bioapplications of C-dots, Carbon 85 (2015) 309–327.
[40] O. Mkhari, T.D. Ntuli, N.J. Coville, E.N. Nxumalo, M.S. Maubane-Nkadimeng, A comparison of fluorescent N-doped carbon dots supported on the surface of hollow and solid carbon spheres, and solid silica spheres, Diamond and Related Materials 118 (2021), 108500.
[41] X. Zhang, S. Wang, C. Zhu, M. Liu, Y. Ji, L. Feng, L. Tao, Y. Wei, Carbon-dots derived from nanodiamond: photoluminescence tunable nanoparticles for cell imaging, Journal of colloid and interface science 397 (2013) 39–44.
[42] J. Liu, T. Kong, H.M. Xiong, Mulberry-leaves-derived red-emissive carbon dots for feeding silkworms to produce brightly fluorescent silk, Advanced Materials 34 (16) (2022), 2200152.
[43] L.M. Shen, J. Liu, New development in carbon quantum dots technical applications, Talanta 156 (2016) 245–256.
[44] Y. Herbani, M.M. Suliyanti, Concentration effect on optical properties of carbon dots at room temperature, Journal of Luminescence 198 (2018) 215–219.
[45] K. Jiang, S. Sun, L. Zhang, Y. Lu, A. Wu, C. Cai, H. Lin, Red, green, and blue luminescence by carbon dots: full-color emission tuning and multicolor cellular imaging, Angewandte Chemie International Edition 54 (18) (2015) 5360–5363.
[46] A. Kundu, B. Park, J. Oh, K.V. Sankar, C. Ray, W.S. Kim, S.C. Jun, Multicolor emissive carbon dot with solvatochromic behavior across the entire visible spectrum, Carbon 156 (2020) 110–118.
[47] Y. Chen, M. Zheng, Y. Xiao, H. Dong, H. Zhang, J. Zhuang, H. Hu, B. Lei, Y. Liu, A self-quenching-resistant carbon-dot powder with tunable solid-state fluorescence and construction of dual-fluorescence morphologies for white light-emission, Advanced Materials 28 (2) (2016) 312–318.
[48] L.L. Mokoloko, B.J. Matsoso, R.P. Forbes, D.H. Barrett, B.D. Moreno, N.J. Coville, Evolution of large-area reduced graphene oxide nanosheets from carbon dots via thermal treatment, Carbon Trends 4 (2021), 100074.
[49] S.Y. Lim, W. Shen, Z. Gao, Carbon quantum dots and their applications, Chemical Society Reviews 44 (1) (2015) 362–381.
[50] R. Liu, D. Wu, S. Liu, K. Koynov, W. Knoll, Q. Li, An aqueous route to multicolor photoluminescent carbon dots using silica spheres as carriers, Angewandte Chemie International Edition 48 (25) (2009) 4598–4601.
[51] J.F.Y. Fong, Y.H. Ng, S.M. Ng, Carbon dots as a new class of light emitters for biomedical diagnostics and therapeutic applications, Fullerenes, Graph. Nanotub. (2018) 227–295.
[52] J. Chen, J. Liu, J. Li, L. Xu, Y. Qiao, One-pot synthesis of nitrogen and sulfur co-doped carbon dots and its application for sensor and multicolor cellular imaging, Journal of Colloid and Interface Science 485 (2017) 167–174.
[53] Z. Ma, H. Ming, H. Huang, Y. Liu, Z. Kang, One-step ultrasonic synthesis of fluorescent N-doped carbon dots from glucose and their visible-light sensitive photocatalytic ability, New Journal of Chemistry 36 (4) (2012) 861–864.
[54] H. Ding, X.H. Li, X.B. Chen, J.S. Wei, X.B. Li, H.M. Xiong, Surface states of carbon dots and their influences on luminescence, Journal of Applied Physics 127 (23) (2020), 231101.
[55] M. Zhang, Q. Yao, W. Guan, C. Lu, J.M. Lin, Layered double hydroxide-supported carbon dots as an efficient heterogeneous Fenton-like catalyst for generation of hydroxyl radicals, The Journal of Physical Chemistry C 118 (19) (2014) 10441–10447.
[56] R.R. Pandey, C.C. Chusuei, Carbon nanotubes, graphene, and carbon dots as electrochemical biosensing composites, Molecules 26 (21) (2021) 6674.
[57] Y. Liu, S. Roy, S. Sarkar, J. Xu, Y. Zhao, J. Zhang, A review of carbon dots and their composite materials for electrochemical energy technologies, Carbon Energy 3 (5) (2021) 795–826.
[58] R.S. Sahu, A. Dubey, Y.H. Shih, Novel metal-free in-plane functionalized graphitic carbon nitride with graphene quantum dots for effective photodegradation of 4-bromophenol, Carbon 182 (2021) 89–99.
[59] F. Liao, Y. Shi, Q. Dang, H. Yang, H. Huang, Z. Kang, M. Shao, Carbon dots dominated photoelectric surface in titanium dioxide nanotube/nitrogen-doped carbon dot/gold nanocomposites for improved photoelectrochemical water splitting, Journal of Colloid and Interface Science 606 (2022) 1274–1283.
[60] Z. Mou, C. Lu, K. Yu, H. Wu, H. Zhang, J. Sun, M. Zhu, M. Cynthia Goh, Chemical interaction in nitrogen-doped graphene quantum dots/graphitic carbon nitride heterostructures with enhanced photocatalytic H2 evolution, Energy Technology 7 (3) (2019), 1800589.

[61] F. Yan, H. Zhang, J. Xu, Y. Wu, Y. Zang, J. Sun, Color emission carbon dots with quench-resixastant solid-state fluorescence for light-emitting diodes, ACS Sustainable Chemistry & Engineering 9 (10) (2021) 3901–3908.
[62] R.J. Fan, Q. Sun, L. Zhang, Y. Zhang, A.H. Lu, Photoluminescent carbon dots directly derived from polyethylene glycol and their application for cellular imaging, Carbon 71 (2014) 87–93.
[63] W. Gao, Y. Ma, Y. Zhou, H. Song, L. Li, S. Liu, X. Liu, B. Gao, C. Liu, K. Zhang, High photoluminescent nitrogen-doped carbon dots with unique double wavelength fluorescence emission for cell imaging, Materials Letters 216 (2018) 84–87.
[64] X. Chu, Y. Liu, P. Zhang, K. Li, W. Feng, B. Sun, N. Zhou, J. Shen, Silica-supported near-infrared carbon dots and bicarbonate nanoplatform for triple synergistic sterilization and wound healing promotion therapy, Journal of Colloid and Interface Science 608 (2022) 1308–1322.
[65] M. Fang, A.N.C. Neto, L. Fu, R.A. Ferreira, V. deZeaBermudez, L.D. Carlos, A hybrid materials approach for fabricating efficient WLEDs based on di-ureasils doped with carbon dots and a europium complex, Advanced Materials Technologies 7 (3) (2022), 2100727.
[66] W.K. Li, J. Zhang, S. Wang, Z.Q. Ma, J.T. Feng, H.W. Pei, Y.M. Liu, Simultaneous determination of three herbicide residues in wheat flour based on the hollow fiber supported carbon dots, Journal of Food Composition and Analysis 108 (2022), 104426.
[67] H. Luo, S. Dimitrov, M. Daboczi, J.S. Kim, Q. Guo, Y. Fang, M.A. Stoeckel, P. Samori, O. Fenwick, A.B. Jorge Sobrido, X. Wang, Nitrogen-doped carbon dots/TiO2 nanoparticle composites for photoelectrochemical water oxidation, ACS Applied Nano Materials 3 (4) (2020) 3371–3381.
[68] J. Sun, H. Maimaiti, B. Xu, L. Feng, J. Bao, X. Zhao, Photoelectrocatalytic degradation of wastewater and simultaneous hydrogen production on copper nanorod-supported coal-based N-carbon dot composite nanocatalysts, Applied Surface Science 585 (2022), 152701.
[69] S. Xu, H. Liu, A. Long, H. Li, C. Chen, S. Feng, J. Fan, Carbon dot-decorated graphite carbon nitride composites for enhanced solid-phase microextraction of chlorobenzenes from water, Nanomaterials 12 (3) (2022) 335.
[70] V.B. Kumar, D. Kashyap, H. Teller, M.G. Gebru, A. Gedanken, A. Schechter, Methyl formate and dimethyl ether electro-oxidation on PtPdSn catalyst supported on carbon nanotube decorated with carbon dots, Materials Today Sustainability 17 (2022), 100095.
[71] F. Liao, Y. Shi, Q. Dang, H. Yang, H. Huang, Z. Kang, M. Shao, Carbon dots dominated photoelectric surface in titanium dioxide nanotube/nitrogen-doped carbon dot/gold nanocomposites for improved photoelectrochemical water splitting, Journal of Colloid and Interface Science 606 (2022) 1274–1283.
[72] S. Kainth, V. Sharma, M. Bhagat, S. Basu, Yellow emissive carbon dots in ludox silica matrix with anticancer activity for enhanced imaging of developed sweat latent fingermarks, Materials Today Chemistry 23 (2022), 100659.
[73] A. Velumani, P. Sengodan, P. Arumugam, R. Rajendran, S. Santhanam, M. Palanisamy, Carbon quantum dots supported ZnO sphere based photocatalyst for dye degradation application, Current Applied Physics 20 (10) (2020) 1176–1184.
[74] G. Jiang, H. Liu, J. Liu, L.E. Liu, Y. Li, L. Xue, Y. Wu, R. Yang, Engineering of multifunctional carbon nanodots-decorated plasmonic Au@ Ag nanoenzymes for photoelectrochemical biosensing of microRNA-155, Sensors and Actuators B: Chemical 360 (2022), 131653.
[75] Y. Han, J. Wu, Y. Li, X. Gu, T. He, Y. Zhao, H. Huang, Y. Liu, Z. Kang, Carbon dots enhance the interface electron transfer and photoelectrochemical kinetics in TiO2 photoanode, Applied Catalysis B: Environmental 304 (2022), 120983.
[76] A.T.N. Nguyen, J.H. Shim, All carbon hybrid N-doped carbon dots/carbon nanotube structures as an efficient catalyst for the oxygen reduction reaction, RSC advances 11 (21) (2021) 12520–12530.
[77] J. Zhuang, S. Ren, B. Zhu, C. Han, Y. Li, X. Zhang, H. Gao, M. Fan, Q. Tian, Lignin-based carbon dots as high-performance support of Pt single atoms for photocatalytic H2 evolution, Chemical Engineering Journal 446 (2022), 136873.
[78] P. Xu, Z. Nan, A. Zhu, Z. Gu, A facile method for preparation of hollow mesoporous silica sphere and its application, Materials Letters 205 (2017) 20–23.
[79] H. Zhang, X. Qiao, T. Cai, J. Chen, Z. Li, H. Qiu, Preparation and characterization of carbon dot-decorated silica stationary phase in deep eutectic solvents for hydrophilic interaction chromatography, Analytical and bioanalytical chemistry 409 (9) (2017) 2401–2410.
[80] Z. Guo, Z. Zhu, X. Zhang, Y. Chen, Facile synthesis of blue-emitting carbon dots@ mesoporous silica composite spheres, Solid State Sciences 76 (2018) 100–104.
[81] L. He, H. Zhang, H. Fan, X. Jiang, W. Zhao, G.Q. Xiang, Carbon-dot-based dual-emission silica nanoparticles as a ratiometric fluorescent probe for vanadium (V) detection in mineral water samples, Spectrochimica Acta Part A: Molecular and Biomolecular Spectroscopy 189 (2018) 51–56.
[82] H. Rao, W. Liu, Z. Lu, Y. Wang, H. Ge, P. Zou, X. Wang, H. He, X. Zeng, Y. Wang, Silica-coated carbon dots conjugated to CdTe quantum dots: a ratiometric fluorescent probe for copper (II), Microchimica Acta 183 (2) (2016) 581–588.
[83] D.A. Eurov, E.Y. Stovpiaga, D.A. Kurdyukov, A.A. Dukin, A.N. Smirnov, V. G. Golubev, Luminescent properties of carbon nanodots bound to the surface of spherical microresonator, Physics of the Solid State 62 (10) (2020) 1898–1904.
[84] H. Zhang, X. Qiao, T. Cai, J. Chen, Z. Li, H. Qiu, Preparation and characterization of carbon dot-decorated silica stationary phase in deep eutectic solvents for hydrophilic interaction chromatography, Analytical and bioanalytical chemistry 409 (9) (2017) 2401–2410.
[85] N. Massad-Ivanir, S.K. Bhunia, N. Raz, E. Segal, R. Jelinek, Synthesis and characterization of a nanostructured porous silicon/carbon dot-hybrid for orthogonal molecular detection, NPG Asia Materials 10 (1) (2018) e463, e463.
[86] Y. Liu, C.Y. Liu, Z.Y. Zhang, W.D. Yang, S.D. Nie, Plasmon-enhanced photoluminescence of carbon dots–silica hybrid mesoporous spheres, Journal of Materials Chemistry C 3 (12) (2015) 2881–2885.
[87] S. Pandey, A. Mewada, M. Thakur, S. Pillai, R. Dharmatti, C. Phadke, M. Sharon, Synthesis of mesoporous silica oxide/C-dot complex (meso-SiO 2/C-dots) using pyrolysed rice husk and its application in bioimaging, RSC Advances 4 (3) (2014) 1174–1179.
[88] E.A. Stepanidenko, P.D. Khavlyuk, I.A. Arefina, S.A. Cherevkov, Y. Xiong, A. Döring, G.V. Varygin, D.A. Kurdyukov, D.A. Eurov, V.G. Golubev, M. A. Masharin, Strongly luminescent composites based on carbon dots embedded in a nanoporous silicate glass, Nanomaterials 10 (6) (2020) 1063.
[89] G.X. Liang, K.R. Zhao, Y.S. He, Z.J. Liu, S.Y. Ye, L. Wang, Carbon dots and gold nanoparticles doped metal-organic frameworks as high-efficiency ECL emitters for monitoring of cell apoptosis, Microchemical Journal 171 (2021), 106787.
[90] L. Xu, M. Pan, G. Fang, S. Wang, Carbon dots embedded metal-organic framework@ molecularly imprinted nanoparticles for highly sensitive and selective detection of quercetin, Sensors and Actuators B: Chemical 286 (2019) 321–327.
[91] H.O. Othman, R. Hassan, A. Faizullah, M. Ghadiri, A carbon-based fluorescent probe (N-CDs) encapsulated in a zeolite matrix (NaFZ) for ultrasensitive detection of Hg (II) in fish, Talanta 234 (2021), 122646.
[92] X. Wang, H. Guo, N. Wu, M. Xu, L. Zhang, W. Yang, A dual-emission fluorescence sensor constructed by encapsulating double carbon dots in zeolite imidazole frameworks for sensing Pb2+, Colloids and Surfaces A: Physicochemical and Engineering Aspects 615 (2021), 126218.
[93] X. Zhan, S. Hu, J. Wang, H. Chen, X. Chen, J. Yang, H. Yang, Z. Su, One-pot electrodeposition of metal organic frameworks composite accelerated by gold nanoparticles and electroreduced carbon dots for electroanalysis of bisphenol A in real plastic samples, Sensors and Actuators B: Chemical 346 (2021), 130499.
[94] H.O. Othman, R. Hassan, A. Faizullah, M. Ghadiri, A carbon-based fluorescent probe (N-CDs) encapsulated in a zeolite matrix (NaFZ) for ultrasensitive detection of Hg (II) in fish, Talanta 234 (2021), 122646.
[95] X. Xu, J. Chen, W. Shi, D. Sun, S. Chu, L. Sun, J. Zhai, J. Pei, L. Wang, S. Ruan, Z. Tang, Synthesis of carbon nanodots in zeolite SAPO-46 channels for Q-switched fiber laser generation, Journal of Alloys and Compounds 782 (2019) 837–844.
[96] N.J. Coville, S.D. Mhlanga, E.N. Nxumalo, A. Shaikjee, A review of shaped carbon nanomaterials, South African Journal of Science 107 (3) (2011) 1–15.
[97] B.K. Kaushik, M.K. Majumder, Carbon Nanotube Based VLSI Interconnects: Analysis and Design, Springer India, New Delhi, 2015, pp. 1–14.
[98] D. Saha, C.L. Heldt, M.F. Gencoglu, K.S. Vijayaragavan, J. Chen, A. Saksule, A study on the cytotoxicity of carbon-based materials, Materials Science and Engineering: C 68 (2016) 101–108.
[99] A. Azari, M. Noorisepehr, E. Dehghanifard, K. Karimyan, S.Y. Hashemi, E. M. Kalhori, R. Norouzi, S. Agarwal, V.K. Gupta, Experimental design, modeling and mechanism of cationic dyes biosorption on to magnetic chitosan-lutaraldehyde composite, International journal of biological macromolecules 131 (2019) 633–645.
[100] H. Yoshida, A. Okamoto, T. Kataoka, Adsorption of acid dye on cross-linked chitosan fibers: equilibria, Chemical Engineering Science 48 (12) (1993) 2267–2272.
[101] J. Xing, X. Wang, J. Xun, J. Peng, Q. Xu, W. Zhang, T. Lou, Preparation of micro-nanofibrous chitosan sponges with ternary solvents for dye adsorption, Carbohydrate polymers 198 (2018) 69–75.
[102] Q. Huang, S. Hu, H. Zhang, J. Chen, Y. He, F. Li, W. Weng, J. Ni, X. Bao, Y. Lin, Carbon dots and chitosan composite film based biosensor for the sensitive and selective determination of dopamine, Analyst 138 (18) (2013) 5417–5423.
[103] M. Omidi, A. Yadegari, L. Tayebi, Wound dressing application of pH-sensitive carbon dots/chitosan hydrogel, RSC advances 7 (18) (2017) 10638–10649.
[104] A. Konwar, N. Gogoi, G. Majumdar, D. Chowdhury, Green chitosan–carbon dots nanocomposite hydrogel film with superior properties, Carbohydrate polymers 115 (2015) 238–245.
[105] X.Y. Dong, X.Q. Niu, Z.Y. Zhang, J.S. Wei, H.M. Xiong, Red fluorescent carbon dot powder for accurate latent fingerprint identification using an artificial intelligence program, ACS applied materials & interfaces 12 (26) (2020) 29549–29555.
[106] K.M. Liew, Z.X. Lei, L.W. Zhang, Mechanical analysis of functionally graded carbon nanotube reinforced composites: a review, Composite Structures 120 (2015) 90–97.
[107] Y. Deng, Y.S. Ok, D. Mohan, C.U. Pittman Jr., X. Dou, Carbamazepine removal from water by carbon dot-modified magnetic carbon nanotubes, Environmental research 169 (2019) 434–444.
[108] Y. Pei, H. Song, Y. Liu, Y. Cheng, W. Li, Y. Chen, Y. Fan, B. Liu, S. Lu, Boron–nitrogen-doped carbon dots on multi-walled carbon nanotubes for efficient electrocatalysis of oxygen reduction reactions, Journal of Colloid and Interface Science 600 (2021) 865–871.
[109] H. Li, Y. Xu, L. Zhao, J. Ding, M. Chen, G. Chen, Y. Li, L. Ding, Synthesis of tiny carbon dots with high quantum yield using multi-walled carbon nanotubes as support for selective "turn-off-on" detection of rutin and Al3+, Carbon 143 (2019) 391–401.
[110] Z.A. Qiao, Q. Huo, M. Chi, G.M. Veith, A.J. Binder, S. Dai, A "ship-in-A-bottle" approach to synthesis of polymer dots@ silica or polymer dots@ carbon core-shell nanospheres, Advanced materials 24 (45) (2012) 6017–6021.
[111] Q.L. Chen, W.Q. Ji, S. Chen, Direct synthesis of multicolor fluorescent hollow carbon spheres encapsulating enriched carbon dots, Scientific reports 6 (1) (2016) 1–8.

[112] L. Luo, J. Ma, H. Zhu, J. Tang, Embedded carbon in a carbon nitride hollow sphere for enhanced charge separation and photocatalytic water splitting, Nanoscale 12 (13) (2020) 7339–7346.
[113] H. Wang, J. Di, Y. Sun, J. Fu, Z. Wei, H. Matsui, C. del, A. Alonso, S. Zhou, Biocompatible PEG-chitosan@ carbon dots hybrid nanogels for two-photon fluorescence imaging, near-infrared light/pH dual-responsive drug carrier, and synergistic therapy, Advanced Functional Materials 25 (34) (2015) 5537–5547.
[114] Y.K. Li, T. Yang, M.L. Chen, J.H. Wang, Supported carbon dots serve as high-performance adsorbent for the retention of trace cadmium, Talanta 180 (2018) 18–24.
[115] F. Abbas, S. Kumar, S.K. Pal, D. Panda, Carbon nanodot doped in polymer film: plasmophore enhancement, catalytic amination and white-light generation, Journal of Molecular Liquids 347 (2022), 118001.
[116] R. Momper, J. Steinbrecher, M. Dorn, I. Rörich, S. Bretschneider, M. Tonigold, C. Ramanan, S. Ritz, V. Mailänder, K. Landfester, M.B. Bannwarth, Enhanced photoluminescence properties of a carbon dot system through surface interaction with polymeric nanoparticles, Journal of colloid and interface science 518 (2018) 11–20.
[117] H. Li, L. Zhao, Y. Xu, T. Zhou, H. Liu, N. Huang, J. Ding, Y. Li, L. Ding, Single-hole hollow molecularly imprinted polymer embedded carbon dot for fast detection of tetracycline in honey, Talanta 185 (2018) 542–549.
[118] H.M. Ahmed, M. Ghali, W. Zahra, M.M. Ayad, Preparation of carbon quantum dots/polyaniline nanocomposite: towards highly sensitive detection of picric acid, Spectrochimica Acta Part A: Molecular and Biomolecular Spectroscopy 260 (2021), 119967.
[119] B. Yu, Y. Wang, M. Sun, Y. Luo, H. Yu, L. Zhang, Preparation of carbon dots-doped terbium phosphonate coordination polymers as ratiometric fluorescent probe for citrate detection, Spectrochimica Acta Part A: Molecular and Biomolecular Spectroscopy 268 (2022), 120656.
[120] M.E. Mahmoud, N.A. Fekry, A.M. Abdelfattah, Removal of uranium (VI) from water by the action of microwave-rapid green synthesized carbon quantum dots from starch-water system and supported onto polymeric matrix, Journal of hazardous materials 397 (2020), 122770.
[121] Y. Zhai, P. Wang, X. Zhang, S. Liu, J. Li, Z. Chen, S. Li, Carbon dots confined in 3D polymer network: producing robust room temperature phosphorescence with tunable lifetimes, Chinese Chemical Letters 33 (2) (2022) 783–787.
[122] J.S. Wei, C. Ding, P. Zhang, H. Ding, X.Q. Niu, Y.Y. Ma, C. Li, Y.G. Wang, H. M. Xiong, Robust negative electrode materials derived from carbon dots and porous hydrogels for high-performance hybrid supercapacitors, Advanced Materials 31 (5) (2019), 1806197.
[123] J.S. Wei, T.B. Song, P. Zhang, X.Q. Niu, X.B. Chen, H.M. Xiong, A new generation of energy storage electrode materials constructed from carbon dots, Materials Chemistry Frontiers 4 (3) (2020) 729–749.
[124] G. Zhang, Q. Ji, Z. Wu, G. Wang, H. Liu, J. Qu, J. Li, Facile “spot-heating” synthesis of carbon dots/carbon nitride for solar hydrogen evolution synchronously with contaminant decomposition, Advanced Functional Materials 28 (14) (2018), 1706462.
[125] X. Jian, X. Liu, H.M. Yang, J.G. Li, X.L. Song, H.Y. Dai, Z.H. Liang, Construction of carbon quantum dots/proton-functionalized graphitic carbon nitride nanocomposite via electrostatic self-assembly strategy and its application, Applied Surface Science 370 (2016) 514–521.
[126] K. Radhakrishnan, S. Sivanesan, P. Panneerselvam, Turn-On fluorescence sensor based detection of heavy metal ion using carbon dots@ graphitic-carbon nitride nanocomposite probe, Journal of Photochemistry and Photobiology A: Chemistry 389 (2020), 112204.
[127] D. Chatterjee, S. Dasgupta, Visible light induced photocatalytic degradation of organic pollutants, Journal of Photochemistry and Photobiology C: Photochemistry Reviews 6 (2–3) (2005) 186–205.
[128] L. Ling, C. Wang, M. Ni, C. Shang, Enhanced photocatalytic activity of TiO2/single-walled carbon nanotube (SWCNT) composites under UV-A irradiation, Separation and Purification Technology 169 (2016) 273–278.
[129] Y.Q. Zhang, D.K. Ma, Y.G. Zhang, W. Chen, S.M. Huang, N-doped carbon quantum dots for TiO2-based photocatalysts and dye-sensitized solar cells, Nano Energy 2 (5) (2013) 545–552.
[130] Y. Yang, X. Ji, M. Jing, H. Hou, Y. Zhu, L. Fang, X. Yang, Q. Chen, C.E. Banks, Carbon dots supported upon N-doped TiO 2 nanorods applied into sodium and lithium ion batteries, Journal of Materials Chemistry A 3 (10) (2015) 5648–5655.
[131] H. Yu, Y. Zhao, C. Zhou, L. Shang, Y. Peng, Y. Cao, L.Z. Wu, C.H. Tung, T. Zhang, Carbon quantum dots/TiO 2 composites for efficient photocatalytic hydrogen evolution, Journal of Materials Chemistry A 2 (10) (2014) 3344–3351.
[132] T.T.V. Nu, N.H.T. Tran, P.L. Truong, B.T. Phan, M.T.N. Dinh, V.P. Dinh, T.S. Phan, S. Go, M. Chang, K.T.L. Trinh, V. Van Tran, Green Synthesis of Microalgae-Based Carbon Dots for Decoration of TiO2 Nanoparticles in Enhancement of Organic Dye Photodegradation, vol. 206, Environmental research, 2022, 112631.
[133] X. Wei, C. Wang, S. Ding, K. Yang, F. Tian, F. Li, One-step synthesis of Ag nanoparticles/carbon dots/TiO2 nanotube arrays composite photocatalyst with enhanced photocatalytic activity, Journal of Environmental Chemical Engineering 9 (1) (2021), 104729.
[134] H. Zhao, X. Yu, C.F. Li, W. Yu, A. Wang, Z.Y. Hu, S. Larter, Y. Li, M.G. Kibria, J. Hu, Carbon quantum dots modified TiO2 composites for hydrogen production and selective glucose photoreforming, Journal of Energy Chemistry 64 (2022) 201–208.